

## THE $\epsilon$ CHAMAELEONTIS YOUNG STELLAR GROUP AND THE CHARACTERIZATION OF SPARSE STELLAR CLUSTERS

ERIC D. FEIGELSON,<sup>1,2</sup> WARRICK A. LAWSON,<sup>2</sup> AND GORDON P. GARMIRE<sup>1</sup>

Received 2003 June 6; accepted 2003 August 29

### ABSTRACT

We present the outcomes of a *Chandra X-Ray Observatory* snapshot study of five nearby Herbig Ae/Be (HAeBe) stars that are kinematically linked with the Oph-Sco-Cen association (OSCA). Optical photometric and spectroscopic follow-up was conducted for the HD 104237 field. The principal result is the discovery of a compact group of pre-main-sequence (PMS) stars associated with HD 104237 and its codistant, comoving B9 neighbor  $\epsilon$  Chamaeleontis AB. We name the group after the most massive member. The group has five confirmed stellar systems ranging from spectral type B9 to M5, including a remarkably high degree of multiplicity for HD 104237 itself. The HD 104237 system is at least a quintet, with four low-mass PMS companions in nonhierarchical orbits within a projected separation of 1500 AU of the HAeBe primary. Two of the low-mass members of the group are actively accreting classical T Tauri stars. The *Chandra* observations also increase the census of companions for two of the other four HAeBe stars, HD 141569 and HD 150193, and identify several additional new members of the OSCA. We discuss this work in light of several theoretical issues: the origin of X-rays from HAeBe stars; the uneventful dynamical history of the high-multiplicity HD 104237 system; and the origin of the  $\epsilon$  Cha group and other OSCA outlying groups in the context of turbulent giant molecular clouds. Together with the similar  $\eta$  Cha cluster, we paint a portrait of sparse stellar clusters dominated by intermediate-mass stars 5–10 Myr after their formation.

*Subject headings:* binaries: visual — open clusters and associations: individual (Scorpius-Centaurus) — stars: formation — stars: individual ( $\epsilon$  Chamaeleontis, HD 104237) — stars: pre-main-sequence — X-rays: stars

### 1. INTRODUCTION

While much star formation research has concentrated on the origins of rich stellar clusters and isolated individual stars, it is likely that a significant fraction of stars also form in groups of  $N \sim 10$ –100 stars, which represent an intermediate scale in the hierarchical structure of star formation regions (Clarke, Bonnell, & Hillenbrand 2000; Elmegreen et al. 2000; Adams & Myers 2001; Kroupa & Boily 2002). If their stellar population is drawn from a standard initial mass function (IMF), these stellar groups will typically be dominated by a few 3–30  $M_{\odot}$  stars. These groups may emerge from relatively small molecular clouds, such as found in the Taurus-Auriga cloud complex, or in parts of giant molecular clouds (GMCs), which also produce the rich OB associations. In the latter case, some plausibly will appear dispersed around OB associations, propelled by motions inherited from the natal turbulent molecular material (Feigelson 1996).

Such young stellar groups are often difficult to find, as they are often dynamically unbound, dispersing into the Galactic field within a few million years (Bonnell & Clarke 1999). Study of small stellar groups is thus largely confined to the pre-main-sequence (PMS) phase. Searches have been pursued in two ways. First, excess stellar densities in the neighborhoods of nearby Herbig Ae/Be (HAeBe) stars—

intermediate-mass PMS stars readily identified by their infrared-luminous disks and active accretion—are sought using optical and near-infrared imagery (Aspin & Barsony 1994; Hillenbrand et al. 1995; Testi et al. 1997; Testi, Palla, & Natta 1999; Weinberger et al. 2000). They are often surrounded by small groups of 5–40 lower mass stars, as expected from the IMF.

Second, sparse stellar groups kinematically convergent with the nearest OB association, the Oph-Sco-Cen association (OSCA; this nomenclature is adopted from Blaauw 1991), have been identified (Mamajek, Lawson, & Feigelson 2000; Ortega et al. 2002). These include one compact group—the  $\eta$  Cha cluster, dominated by a B8 star and three A stars (Mamajek, Lawson, & Feigelson 1999; Lawson et al. 2001)—and two dispersed groups—the  $\beta$  Pic moving group, dominated by five A stars (Zuckerman et al. 2001), and the TW Hya association, with a single A star (HR 4796; Song, Bessell, & Zuckerman 2002 and references therein). The locations of these groups in relation to the OSCA are illustrated in Figure 1. Membership of OSCA outlier groups is principally based on a combination of kinematical criteria and elevated X-ray emission, which is a ubiquitous characteristic throughout PMS evolution from Class I protostars through post-T Tauri stars (Feigelson & Montmerle 1999).

In addition to clustering on 0.1–10 pc scales, intermediate-mass stars may be accompanied by bound companions on  $\leq 1000$  AU scales. The stellar multiplicity of older low-mass stars is established to be

$$\text{singles} : \text{binaries} : \text{triples} : \text{quartets} = 57 : 38 : 4 : 1$$

for every 100 stars (Duquennoy & Mayor 1991). A few higher multiplicity field systems are known, such as Castor,

<sup>1</sup> Department of Astronomy and Astrophysics, Pennsylvania State University, University Park, PA 16802; edf@astro.psu.edu.

<sup>2</sup> School of Physical, Environmental, and Mathematical Sciences, University of New South Wales, Australian Defence Force Academy, Canberra ACT 2600, Australia.

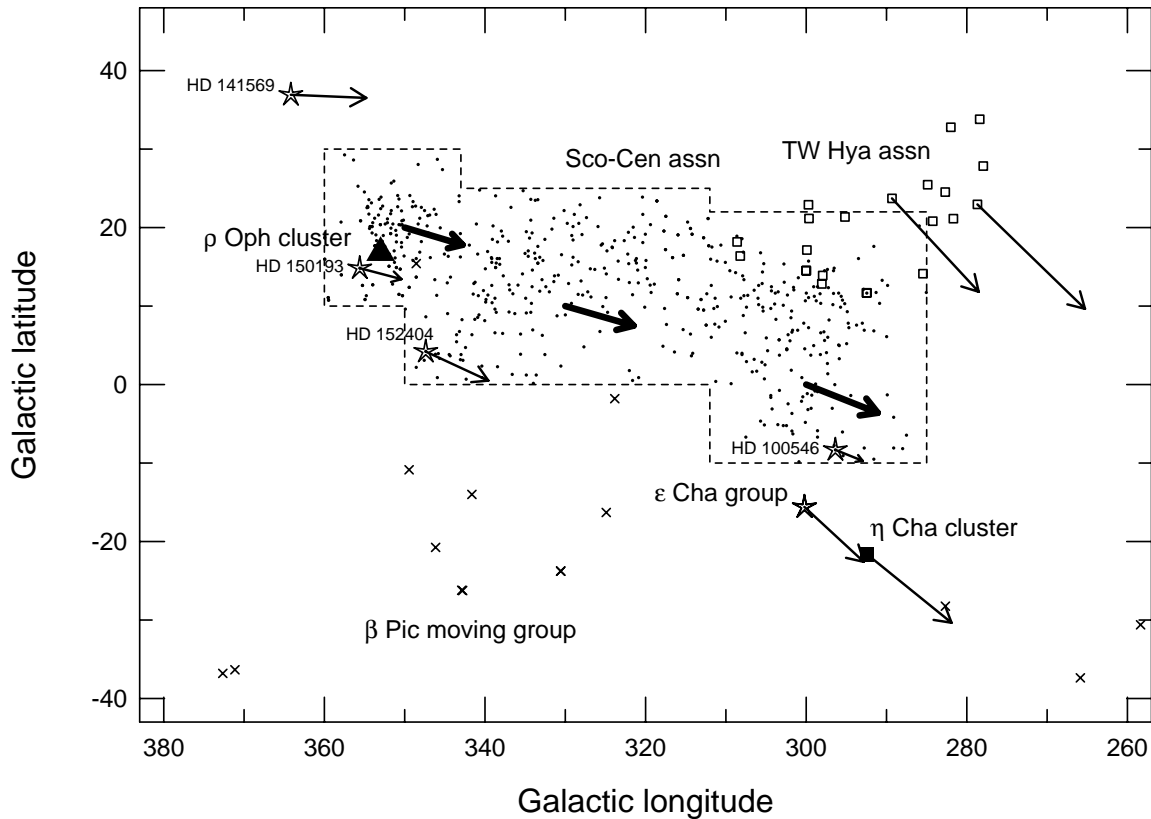


FIG. 1.—The Oph-Sco-Cen association (OSCA) and its comoving stellar groups: the US, UCL, and LCC rich subgroups (*dots in dashed outline*), the  $\rho$  Oph embedded cluster (*triangle*), the TW Hya association (*open squares*), the  $\beta$  Pic moving group (*crosses*), the  $\eta$  Cha cluster (*filled square*), the  $\epsilon$  Cha group (with HD 104237), and the other four H Ae Be systems discussed here (*stars*). Selected proper-motion vectors show displacements over the next 1 Myr.

a sextet of three close binaries dominated by two early A stars. The situation is more confusing for PMS systems. The crowded and rich Orion Nebula cluster simultaneously shows very high multiplicities around its massive OB stars, main-sequence levels of close, lower mass binaries, and a deficiency of wide binaries (Preibisch et al. 1999; Simon, Close, & Beck 1999). The distribution of binary separations may depend on the local density of neighbors even within a single cluster (Brandner & Köhler 1998). In less crowded environments, such as the Taurus-Auriga clouds, binarity is nearly a factor of 2 higher among lower mass PMS systems than in main-sequence stars, so that virtually all stars appear to be born in multiple systems (Mathieu 1994). Binary fractions among H Ae Be stars are also elevated above main-sequence levels, and a few triple systems are known (§ 7.2).

The study of multiplicity in young stars is of critical importance (Zinnecker & Mathieu 2001). It first addresses primordial conditions of star formation, such as the fragmentation of molecular material and redistribution of angular momentum during gravitational collapse (see Klessen 2001, Boss 2002, Larson 2002, and the review by Bodenheimer et al. 2000). But it also reveals subsequent dynamical evolutionary effects, such as the dissipation of molecular material, close stellar encounters, stellar evaporation, and the survival of protoplanetary disks (reviews by Bonnell 2000 and Kroupa 2000).

We report here an effort that combines the two observational approaches outlined above. We seek young, low-mass, PMS stars with elevated X-ray emission around

intermediate-mass PMS H Ae Be stars that are kinematically associated with the OSCA. This is a small study based on only five X-ray snapshots, designed to test the efficacy of the method. Despite the exploratory nature of our effort, one new young OSCA outlying stellar group is found associated with the closely spaced B/A stars  $\epsilon$  Cha and HD 104237 itself. Section 5 details our X-ray, optical/infrared photometric and spectroscopic characterization of the  $\epsilon$  Cha group.<sup>3</sup> We also find new companions within  $\sim 200$  AU of two of the other observed H Ae Be stars, HD 141569 and HD 150193 (§ 6). A variety of theoretical issues are discussed in § 7.

## 2. OUR STRATEGY FOR LOCATING YOUNG STELLAR SYSTEMS

Figure 1 shows  $\simeq \frac{1}{4}$  of the celestial sphere, featuring stars associated with the OSCA. The dashed lines outline the boundaries of the rich Upper Sco (US), Upper Centaurus Lupus (UCL), and Lower Centaurus Crux (LCC) subgroups of the OSCA defined by de Zeeuw et al. (1999) in their detailed study of *Hipparcos* motions. The brighter members, complete to  $V \sim 7$  and consisting mainly of intermediate-mass BAF stars, identified by them are plotted

<sup>3</sup> Following the practice of Mamajek et al. (1999) in naming the  $\eta$  Cha star cluster, we name the new  $\epsilon$  Cha group of PMS stars after the highest mass member. Components HD 104237B–E are named in order of proximity to the primary, HD 104237A.

as small dots. The three thick arrows show subgroup average proper motions during the next 1 Myr without correction for solar reflex motion. *Hipparcos* parallaxes of these bright members establish the subgroup distances to be 145 pc (US), 140 pc (UCL), and 118 pc (LCC).

Several samples of fainter OSCA members within the traditional boundaries have been constructed based on various combinations of kinematical, spectroscopic, and X-ray selection criteria (Preibisch et al. 2002; Mamajek, Meyer, & Liebert 2002), but these constitute only a few percent of the full population of the subgroups, estimated to be  $\approx 6000$  stars with  $M > 0.1 M_{\odot}$ , assuming a standard IMF and some stellar evaporation (de Geus 1992). The late-type members of these samples are particularly valuable in establishing ages from their positions on the PMS tracks in the H-R diagram. The ages for the Oph, US, UCL, and LCC OSCA subgroups are found to be 0–5, 5, 16, and 17 Myr, respectively. This progression of ages led Blaauw (1964, 1991) to suggest that a sequence of distinct star-forming events occurred in the ancestral GMC, where later events are triggered by the shocks and ionization fronts produced by the OB stars of previous events (Elmegreen & Lada 1977). The ages of the outlying OSCA groups are similarly established to be  $\sim 9$ ,  $\sim 12$ , and  $\sim 10$  Myr for the  $\eta$  Cha,  $\beta$  Pic, and TW Hya groups, respectively (Lawson & Feigelson 2001; Zuckerman et al. 2001; Webb et al. 1999).

In this preliminary study, we chose five HAeBe stars with present-day space positions in or near the OSCA and space motions consistent with an origin in the OSCA GMC (Table 1). The first five columns of the table give the star identifiers, *Hipparcos* distances, and estimated masses and ages. See table notes for details.

Column (9) of Table 1 indicates that two of the stars are closely associated with small molecular clouds. HD 100546 is likely associated with the bright-rimmed dark cloud DC 296.2–7.9, located  $0^{\circ}4'$  away (Vieira, Pogodin, & Franco 1999; Mizuno et al. 2001). HD 104237 and its comoving, non-emission line, B9 Vn companion  $\epsilon$  Cha,  $2'$  away, lie among several small molecular clumps with  $M_{\text{gas}} < 1 M_{\odot}$  within  $\sim 10'$  (Knee & Prusti 1996). Knee & Prusti plausibly argue that these are dissipating remnants of the molecular cloud from which these two intermediate-mass stars formed. Indeed, the entire Chamaeleon-Musca region south of the OSCA has many widely dispersed small molecular clouds and filaments,

some closely associated with relatively isolated PMS stars (Mizuno et al. 1998, 2001). These authors (see also Mamajek et al. 2000) discuss the possibility that this molecular material remains after the passage of the interstellar supershells attributed to the OB winds and supernova remnants of the OSCA (de Geus 1992).

Figure 1 qualitatively shows that the five targets have *Hipparcos* proper motions similar to those of the principal OSCA subgroups. Quantitative assessment of an origin in the same molecular cloud complex, which is now largely dispersed, requires accurate radial velocities, which are generally not available. We adopt here the approximate method described by Mamajek et al. (2000; see also Mamajek & Feigelson 2001), where we evaluate the closest approach in three dimensions between a star and OSCA subgroups,  $D_{\text{OSCA}}$ , assuming linear motion and arbitrary radial velocities. This calculation of closest approach includes correction for solar reflex motion and is similar to the measurement of proximity of “spaghetti” in six-dimensional phase space described by Hoogerwerf & Aguilar (1999) and used by de Zeeuw et al. (1999) to establish OSCA memberships. The resulting  $D_{\text{OSCA}}$  distances for the target stars to OSCA subgroup centers over the past 10 Myr are given in the last column of Table 1. In the two cases in which radial velocity measurements are available (HD 141569 and HD 152404; Barbier-Brossat & Figon 2000), our method correctly gives the closest approach to OSCA subgroups for the measured value compared to other hypothetical values.

From this measure of past proximity, available kinematical data for three of the target stars (HD 100546, HD 104237, and HD 150193) are fully consistent with OSCA subgroup membership ( $D_{\text{OSCA}} < 10$  pc), while for two stars (HD 141569 and HD 152404) OSCA membership is less certain ( $D_{\text{OSCA}} \approx 30$  pc). For the three stars lying within the OSCA boundaries (Fig. 1), these results agree with those obtained by de Zeeuw et al. (1999) who assign HD 100546 and HD 150193 as high-probability OSCA members and HD 152404 as a lower probability member.

Finally, we note that for three targets—HD 100546, HD 141569, and HD 150193—searches for close, low-mass companions to the bright HAeBe primary have been made at optical or near-infrared bands (§ 6). This provides us an opportunity to compare the effectiveness of finding companions through X-ray activity *versus* photospheric emission.

TABLE 1  
OBSERVED HAeBe STARS NEAR THE OPH-SCO-CEN ASSOCIATION (OSCA)

HD (1)	Name (2)	R.A. (J2000.0) (3)	Decl. (J2000.0) (4)	Spectral Type (5)	$D$ (pc) (6)	Mass ( $M_{\odot}$ ) (7)	Age (Myr) (8)	Cloud (9)	$D_{\text{OSCA}}$ (pc) (10)
100546 .....	KR Mus	11 33 25.44	−70 11 41.2	B9 Vne	103	2.5	$\geq 10$	Yes	2
104237 .....	DX Cha	12 00 05.08	−78 11 34.5	A0 Vpc	116	2.5	2	Yes	9
141569 .....		15 49 57.75	−03 55 16.4	B9.5e	99	...	$5 \pm 3$	No	35
150193 .....	MWC 863	16 40 17.92	−23 53 45.2	A1 Ve	150	2.3	$> 2$	No	5
152404 .....	AK Sco	16 54 44.85	−36 53 18.6	F5 IVe	145	1.5+1.5	$\sim 6$	No	29

NOTES.—Units of right ascension are hours, minutes, and seconds, and units of declination are degrees, arcminutes, and arcseconds. Properties are obtained from the SIMBAD database except as follows: Masses and ages for HD 100547, HD 104237, and HD 150193 are obtained from their H-R diagram locations by van den Ancker et al. 1997. The age for HD 141569 is from the H-R diagram of its low-mass companions by Weinberger et al. 2000. Spectral types, mass, and age estimates for AK Sco are obtained from the binary orbit analysis of Andersen et al. 1989. The “Cloud” column denotes whether an optical dark cloud or molecular material is found near the star.  $D_{\text{OSCA}}$  gives the closest approach of the star to the UCL or LCC subgroups of the OSCA during the past 5–15 Myr. These last two columns are discussed in § 2.

## 3. CHANDRA OBSERVATIONS AND ANALYSIS

Table 2 gives the log of X-ray observations. We used the  $16' \times 16'$  Advanced CCD Imaging Spectrometer Imager (ACIS-I) array on board the *Chandra X-Ray Observatory*. The satellite and instrument are described by Weisskopf et al. (2002). The first stages of data reduction are described in the Appendix of Townsley et al. (2003). Briefly, we start with the level 1 events from the satellite telemetry, correct event energies for charge transfer inefficiency, and apply a variety of data selection operations, such as *ASCA* event grades and energies in the range 0.5–8 keV. A small (typically  $\sim 1''$ ) correction to the image boresight is made so the X-ray–bright HAeBe stellar position agrees with the *Hipparcos* position.

Candidate sources were located using a wavelet-based detection algorithm (Freeman et al. 2002). We applied a low threshold ( $P = 1 \times 10^{-5}$ ) so that some spurious sources were found, which we excluded later. The image was visually examined for additional sources, such as close companions to the bright HAeBe star. Events for each candidate source were extracted using the *acis\_extract*<sup>4</sup> procedures, which take into account the position-dependent point-spread function. Background is negligible for sources of interest in these short exposures and was not subtracted. Candidate sources with fewer than 3 extracted counts were now rejected.

The valid sources are cross-correlated with the USNO-B1.0 star catalog derived from all-sky Schmidt survey photographic plates (Monet et al. 2003). Sources with counterparts brighter than 16.0 mag in the *B*, *V*, or *R* band are considered to be prime candidate young stars. This criterion eliminates virtually all X-ray sources that are extragalactic. The X-ray sources with stellar counterparts are listed in Tables 3 and 4.

Table 5 provides results from subsequent analysis of the X-ray properties of the sources most likely associated with PMS stars. The following software packages were used: CIAO, version 2.3, and *acis\_extract* for photon extraction; XRONOS, version 5.19, for variability; and XSPEC, version 11.2, for spectral modeling.  $C_{\text{extr}}$  events were extracted in the 0.5–8 keV band from a circular region of radius  $R_{\text{extr}}$  (in arcseconds). The parameter  $f_{\text{PSF}}$  gives the fraction of a point-spread function lying within that radius at the source's location in the ACIS field.<sup>5</sup>

The distribution of photon energies was modeled as emission from a thermal plasma with energy  $kT$  based on MEKAL emissivities (Kaastra & Mewe 2000). For two of the stronger sources, a two-temperature plasma model was needed. For the weaker sources with  $C_{\text{extr}} \leq 30$  counts, the derived  $kT$ -values were unreliable and are provided only to indicate how broadband luminosities were derived. With one exception (HD 104237E), successful fits were found without intervening absorption by interstellar or circum-

TABLE 2  
LOG OF *Chandra* OBSERVATIONS

HD	Observation Date	Exposure (ks)
100546 .....	2002 Feb 4	5.2
104237 .....	2001 Jun 5	3.0
	2002 Feb 4	2.8
141569 .....	2001 Jun 23	2.9
150193 .....	2001 Aug 19	2.9
152404 .....	2001 Aug 19	3.1

stellar material. While the derived plasma energies are often imprecise, broadband fluxes integrated over the best-fit model are insensitive to spectral fitting uncertainties and have roughly  $1/(C_{\text{extr}})^{1/2}$  errors. X-ray luminosities,  $L_s$  in the soft 0.5–2 keV band and  $L_t$  in the total 0.5–8 keV band, are obtained from these fluxes by multiplying by  $4\pi d^2$ , using the distances in Table 1 and dividing by  $f_{\text{PSF}}$ .

Variability information is limited by our short exposures. No source exhibited significant variations within an observation, as measured with a Kolmogorov-Smirnov one-sample test. Virtually all stellar sources observed in the two widely separate exposures of the  $\epsilon$  Cha–HD 104237 field showed long-term variability. Table 5 gives these luminosities separately, assuming no variations in spectral shape.

## 4. OPTICAL OBSERVATIONS

4.1. Color-Magnitude Photometric Study of the  $\epsilon$  Cha–HD 104237 Field

Optical color-magnitude diagrams are a powerful tool aiding the discovery and characterization of PMS stellar populations (Walter et al. 2000; Lawson et al. 2001). For nearby compact, coeval, and codistant groups, PMS stars form an isochrone that is elevated in magnitude above the vast majority of field stars owing to a combination of youth, proximity, and (for groups dispersed from their parent molecular cloud) the absence of significant reddening. For X-ray–discovered groups of PMS stars, such as the  $\eta$  Cha cluster (Mamajek et al. 1999) and the  $\epsilon$  Cha group announced here, optical photometric study also permits an independent evaluation of completeness within the X-ray field (except for low-mass stars located very close to the bright A and B stars). X-ray–faint stars with photometric properties similar to those of X-ray–selected cluster members can be identified and subsequently observed using spectroscopy for confirmation of membership; e.g., for the  $\eta$  Cha cluster, we identified two X-ray–faint late-type members residing within the *ROSAT* High Resolution Imager discovery field, including the strongest disk source in the cluster (Lawson et al. 2002; Lyo et al. 2003b).

We made a map covering most of the *Chandra*  $\epsilon$  Cha–HD 104237 field in the Cousins *VI* photometric bands using the 1.0 m telescope and SITE CCD detector at the Sutherland field station of the South African Astronomical Observatory (SAAO) during 2002 January. Some later *VRI* observations were made in 2002 April and 2003 April to complete coverage of the field. A total field of  $\approx 300$  arcmin<sup>2</sup> centered on HD 104237 was surveyed under photometric conditions in  $\approx 1''.5$  seeing, with the observations transformed to the standard system using observations of

<sup>4</sup> The description and code for *acis\_extract* are available at [http://www.astro.psu.edu/xray/docs/TARA/ae\\_users\\_guide.html](http://www.astro.psu.edu/xray/docs/TARA/ae_users_guide.html).

<sup>5</sup> These values are derived from the 1999 memo “An Analysis of the ACIS-HRMA Point Response Function,” by A. Ware and B. R. McNamara, available at [http://cxc.harvard.edu/cal/Acis/Cal\\_prods/psf/Memo/abstract.html](http://cxc.harvard.edu/cal/Acis/Cal_prods/psf/Memo/abstract.html), and its associated data products. The sub-arcsecond on-axis values were derived from calibration run H-IAI-CR-1.001 and are not very certain, because the point-spread function under in-flight conditions may differ slightly from that seen during ground calibration.

TABLE 3  
MEMBERSHIP OF THE  $\epsilon$  CHA GROUP

Member (1)	ID Type (2)	R.A. (3)	Decl. (4)	Ref. (5)	Name (6)	$\Delta_{RA}$ (arcsec) (7)	$\Delta_{Dec}$ (arcsec) (8)	$V$ (9)	$R$ (10)	$I$ (11)	$J$ (12)	$H$ (13)	$K$ (14)	Spectral Type (15)	$H\alpha$ (Å) (16)	$L_i$ (Å) (17)	Class (18)
1.....	psx	11 59 08.0	-78 12 32.2	1	CXOU J115908.2-781232	+0.0	+0.0	16.99	15.57	13.83	12.01	11.45	11.17	M5	-6.2	+0.9	WTT
2.....	a	11 59 37.6	-78 13 18.6	2	$\epsilon$ Cha AB	...	...	4.90 <sup>a</sup>	...	...	5.02	5.04	4.98	B9 Vn <sup>a</sup>	+13	...	AB
3.....	x	12 00 03.6	-78 11 31.0	3	HD 104237C	...	...	...	...	...	...	...	...	K:	...	...	...
4.....	x	12 00 04.0	-78 11 37.0	3	HD 104237B	...	...	...	...	...	...	...	...	A0 Vpe <sup>a</sup>	-20	...	H AeBe
5.....	asx	12 00 05.1	-78 11 34.6	2	HD 104237A	0.0	0.0	6.59 <sup>a</sup>	...	...	5.81	5.25	4.59	M3	-3.9	+0.6	WTT
6.....	psx	12 00 08.3	-78 11 39.5	1	HD 104237D	+0.0	+0.0	14.28	13.09	11.62	...	...	...	K2	-4.5	+0.5	CTT
7.....	psx	12 00 09.3	-78 11 42.4	1	HD 104237E	+0.0	+0.1	12.08 <sup>b</sup>	11.25 <sup>b</sup>	10.28 <sup>b</sup>	...	...	...	M5	-23	+0.6	CTT
8.....	ps	12 01 44.4	-78 19 26.7	1	USNO-B 120144.7-781926	...	...	17.18 <sup>b</sup>	15.61 <sup>b</sup>	13.72 <sup>b</sup>	11.68	11.12	10.78	M5	-7.8	+0.6	WTT
9.....	psx	12 01 52.5	-78 18 41.3	1	CXOU J120152.8-781840	-0.9	+0.4	16.78	15.29	13.52	11.63	11.04	10.77	M5	-7.8	+0.6	WTT
Confirmed Members																	
Nonmembers																	
x	x	11 59 48.1	-78 11 45.0	2	CPD -77°773	-0.1	+0.0	8.87	...	7.53	6.59	5.98	5.85	K0	+1.2	<0.05	...
x	x	12 00 49.5	-78 09 57.2	2	CPD -77°775	-0.2	+0.2	9.62	...	9.13	8.77	8.61	8.54	F0	+10	<0.05	...
x	x	12 01 18.1	-78 02 52.2	1	CXOU J120118.2-780252	+0.6	+1.4	15.58	14.62	13.80	12.53	11.84	11.61	K7	-1.5	<0.05	...
x	x	11 59 42.0	-78 18 36.6	1	CXOU J115942.2-781836	+0.6	+1.1	18.25	17.74	17.22	16.46	15.85	<16.08	...	...	...	...
x	x	12 01 01.4	-78 06 18.0	4	CXOU J120101.4-780618	+2.4	-1.9	18.82	18.35	17.88	...	...	...	...	...	...	...
x	x	12 01 35.3	-78 04 27.6	4	CXOU J120135.3-780427	-0.3	+1.1	19.61	19.07	18.42	...	...	...	...	...	...	...
p	p	11 58 16.0	-78 08 24.5	1	USNO-B 115816.0-780824	...	...	12.00	...	10.57	9.51	8.84	8.72	K0	+1.0	<0.05	...
p	p	11 58 40.3	-78 12 29.2	1	USNO-B 115840.3-781229	...	...	13.04	...	11.37	10.19	9.47	9.24	K2	+1.1	<0.05	...
p	p	12 02 23.1	-78 05 44.6	1	USNO-B 120223.1-780544	...	...	15.38	...	12.84	11.26	10.32	10.04	M3	+1.2	<0.05	...

NOTE.—Col. (1): Running number used in § 5. Col. (2): a = astrometric; p = photometric; s = spectroscopic; x = X-ray. Col. (5): Position references: (1) 2MASS all-sky catalog; (2) *Hipparcos* and Tycho catalogs; (3) *Chandra* X-ray position aligned to the *Hipparcos* position of HD 104237A; (4) USNO-B1.0 catalog. Cols. (7)–(8): Positional offsets:  $\Delta_{RA}$  and  $\Delta_{Dec}$  are 2MASS (or USNO-B1.0 if 2MASS is unavailable) positions minus X-ray positions. For positive offsets, the X-ray source is southwest of the star. Cols. (9)–(11): Our  $VRI$  photometry from SAAO, except where noted. Cols. (12)–(14): 2MASS  $JHK$  photometry. Col. (15): Spectral types evaluated from our MISSO spectroscopy, except where noted. Cols. (16)–(17):  $H\alpha$  and  $L_i$   $\lambda$ 6707 EWs in angstroms, where a negative value is in emission, obtained from our MISSO spectroscopy (Fig. 3). Col. (18): AB = A or B non-emission-line star; H AeBe = Herbig AB emission-line star; CTT = classical emission-line T Tauri star; WTT = weak-lined T Tauri star.

<sup>a</sup> Bright star data from SIMBAD.

<sup>b</sup> Variable star. Maximum light values listed.

TABLE 4  
CANDIDATE NEW X-RAY-SELECTED OSCA MEMBERS

FIELD	<i>Chandra</i>					CATALOG PHOTOMETRY						NOTES
	R.A. (J2000.0)	Decl. (J2000.0)	$\Delta_{RA}$	$\Delta_{Decl}$	Counts	<i>B</i>	<i>R</i>	<i>I</i>	<i>J</i>	<i>H</i>	<i>K</i>	
HD 100546.....	11 33 39.6	-70 08 05.5	+0.5	-0.2	99	13.9	13.7	12.2	11.33	10.68	10.54	A
	11 33 42.6	-70 21 09.4	+0.6	-0.4	82	13.6	12.9	11.8	11.27	10.86	10.78	
	11 33 43.7	-70 16 25.9	-0.1	-1.4	17	15.7	14.7	14.0	12.68	12.09	11.93	
	11 34 11.8	-70 19 37.7	+0.7	-1.0	13	15.3	14.1	12.9	12.04	11.47	11.36	
	11 34 27.4	-70 13 21.5	-0.3	+0.2	21	13.6	13.3	12.9	11.74	11.38	11.26	
HD 141569.....	...	...	...	...	...	...	...	...	...	...	...	B
HD 150193.....	16 39 45.5	-24 02 02.7	-1.0	-1.3	111	18.0	14.0	14.3	10.17	8.66	7.63	
HD 152404.....	16 40 31.3	-23 49 15.1	+2.3	-1.4	27	17.7:	15.6	13.7	...	...	...	C
	16 54 16.9	-36 56 22.0	-1.4	+2.3	4	16.6	14.8	13.5	12.80	12.06	11.87	D
HD 152404.....	16 54 30.8	-36 49 24.4	+0.3	+0.6	54	10.4	10.0	9.8	9.41	9.33	9.28	E
	16 55 10.2	-36 51 20.2	+4.5	-4.9	8	16.7	14.2	13.8	12.42	11.56	11.29	F

NOTES.—Right ascension and declination are from the wavelet-based source detection algorithm applied to the *Chandra* ACIS image after astrometric alignment of the field to the HAeBe star. Units of right ascension are hours, minutes, and seconds, and units of declination are degrees, arcminutes, and arcseconds. Sources should be designated CXOU J113339.6–700805 and so forth.  $\Delta_{RA}$  and  $\Delta_{Decl}$  are offsets in arcseconds between the 2MASS position and the X-ray source. “Counts” are ACIS counts in a  $\approx 90\%$  extraction region. *BRI* photometry is from the USNO-B1.0 catalog, and *JHK* photometry is from the 2MASS All-Sky Catalog. Mean values are listed when two epochs are given in the USNO-B1.0 catalog.

“NOTES” COLUMN.—(A) A second X-ray source is present  $8''$  to the southeast of this source. (B) This heavily reddened but luminous star is identified with IRAS 16367–2356, which has flux densities of 1.2, 1.9, and 3.3 Jy in the 12, 25, and 60  $\mu\text{m}$  bands, respectively. Weintraub 1990 classifies the star as a “possible classical T Tauri” on the basis of  $H\alpha$  emission. The star lies  $10'$  south of the HAeBe star, and the field is at the northern edge of a several-degree line of Lynds dark clouds between L1712 around  $16^{\text{h}}38^{\text{m}}$ ,  $-24^{\circ}26'$  and L1729 around  $16^{\text{h}}43^{\text{m}}$ ,  $-24^{\circ}05'$  (J2000.0). These are long, cometary-like clouds blown eastward of the  $\rho$  Oph cloud cores by OSCA US OB stars (Loren 1989). (C) The larger-than-average  $2.7''$  offset between the X-ray and 2MASS positions is acceptable for a faint source lying  $7'$  off-axis of the ACIS aim point. This low-mass star lies  $10''$  northeast of a much more luminous but reddened star with  $B = 14.9$ ,  $I = 10.7$ ,  $J = 9.30$ ,  $H = 8.38$ , and  $K = 8.04$ . We suggest that these two stars comprise a wide binary system and that both are PMS members of the OSCA. (D) This is a marginal ACIS source. (E) HD 152368, an unstudied B9 V star at the southern edge of OSCA UCL region. A  $K = 14.0$  companion lies  $8.8''$  to the southeast. We suggest that these are a new high- and low-mass member of the OSCA, respectively, and that HD 152368 might itself be an unresolved binary with a late-type companion responsible for the X-ray emission. HD 152368 is missing from the OSCA membership list of de Zeeuw et al. 1999 because it was not in the *Hipparcos* Input Catalog and thus has no parallax. (F) This is a somewhat confused area, with four stars within  $10''$  of the X-ray position and USNO-B1.0/2MASS position discrepancies up to  $3''$ . The ACIS source is faint and  $7'$  off-axis, so that its position is uncertain by  $\approx 3''$ . Here we tentatively associate the X-ray source with the brightest of the stars.

TABLE 5  
X-RAY PROPERTIES OF CONFIRMED PMS STARS

Member	Source	Epoch	$C_{\text{extr}}$	$R_{\text{extr}}$ (arcsec)	$f_{\text{PSF}}$	$kT$ (keV)	$\log L_s$ (ergs $\text{s}^{-1}$ )	$\log L_r$ (ergs $\text{s}^{-1}$ )
$\epsilon$ Cha–HD 104237 Field								
1.....	CXOU J115908.0–781232	1	10	4.0	0.90	0.3	28.6	...
		2	4	4.0	0.90	0.3	28.2	...
3.....	HD 104237C	1	0	1.0	0.60	0.9	<28.2	...
		2	6	1.0	0.60	0.9	28.5	...
4.....	HD 104237B	1	18	0.50	0.15	1	29.1	...
		2	26	0.50	0.15	1	29.2	...
5.....	HD 104237A	1	299	0.75	0.40	0.7/5.2 <sup>a</sup>	30.2	30.4
		2	340	0.75	0.40	0.7/5.2 <sup>a</sup>	30.2	30.5
6.....	HD 104237D	1	37	1.0	0.60	0.6	29.4	...
		2	33	1.0	0.60	0.6	29.3	...
7.....	HD 104237E	1	25	1.0	0.60	2.0 <sup>b</sup>	28.6 <sup>b</sup>	29.9 <sup>b</sup>
		2	198	1.0	0.60	2.0 <sup>b</sup>	29.5 <sup>b</sup>	30.8 <sup>b</sup>
9.....	CXOU J120152.5–781841	1	14	7.5	0.75	1	28.5	...
		2	7	7.5	0.75	1	28.2	...
Other Fields								
	HD 100546	1	59	2.5	0.75	2.5	29.2	29.4
	HD 141569A	1	161	1.0	0.60	0.7/4.5 <sup>a</sup>	29.9	30.1
	HD 141569D	1	49	0.5	0.15	1.0	29.9	...
	HD 150193A	1	152	1.0	0.60	5.0	30.2	30.7
	HD 150193C	1	13	0.5	0.15	0.8	29.6	...
	HD 152404	1	17	2.5	0.75	0.4	29.1	...

<sup>a</sup> Two-temperature plasma fits were required to model this X-ray spectrum.

<sup>b</sup> This spectrum showed significant soft X-ray absorption, with  $\log N_{\text{H}} = 22.4 \pm 0.1 \text{ cm}^{-2}$ . The inferred intrinsic luminosities corrected for this absorption are 6 (3) times higher in the 0.5–2 (0.5–8) keV band than the observed values given here.

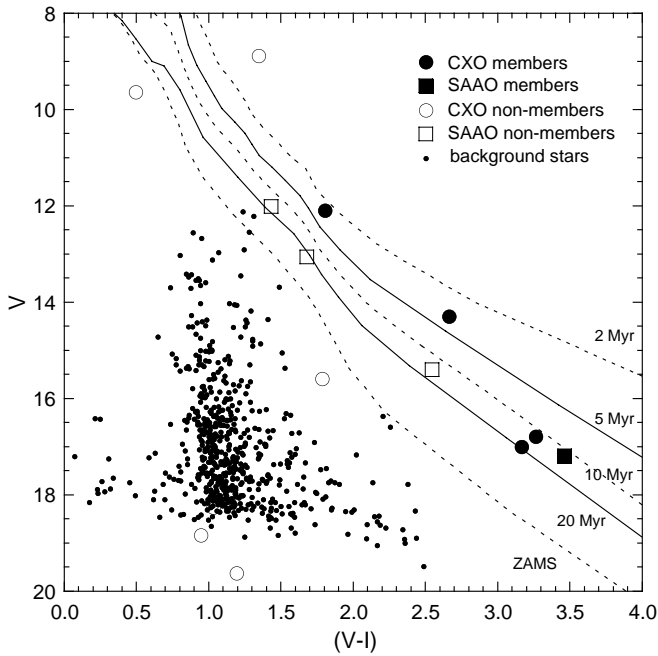


FIG. 2.— $V-I$  vs.  $V$  color-magnitude diagram for the  $\epsilon$  Cha group. Large filled symbols are for confirmed PMS stars resulting from optical spectroscopic study of *Chandra* detections (filled circles) and those resulting from ground-based photometric study (filled square). The large open symbols indicate *Chandra* and photometric candidates not found to be PMS. The small circles are for representative background stars. The model isochrones (units of Myr) are from Siess, Dufour, & Forestini (2000).

southern photometric standard stars. Exposure times in the  $VRI$  bands of 90, 60, and 30 s, respectively, permit detection—for  $\sim 10$  Myr old PMS stars at  $\sim 100$  pc distance—down to M6 spectral type cluster members with  $V \approx 18$  and  $V-I \approx 4.5$ . For the central regions of the *Chandra* field, we also obtained exposures of shorter duration (1–30 s) to minimize saturation effects from the bright  $\epsilon$  Cha and HD 104237 on photometry of several spatially proximate late-type stars. Finally, we obtained deeper exposures ( $VRI$  exposures of 900, 600, and 300 s) to characterize the optical counterparts of the faintest *Chandra* sources.

Figure 2 shows the placement of X-ray–selected stars from the *Chandra* field (Table 3) in the  $V-I$  versus  $V$  color-magnitude diagram (large circles), along with several hundred X-ray–faint field stars representative of background sources in the shallow  $VI$  survey. The symbols used for these and other stars reflect the outcomes of photometric and spectroscopic studies that we detail in the following sections. We compare the location of these stars to isochrones from the PMS evolutionary models of Siess et al. (2000) scaled to a distance of 114 pc, the mean of *Hipparcos* distances to  $\epsilon$  Cha ( $112 \pm 7$  pc) and HD 140237 ( $116 \pm 8$  pc). The location of the *Chandra* stellar counterparts in the color-magnitude diagram is our first evidence for stellar youth in the X-ray–bright stars located nearby  $\epsilon$  Cha and HD 140237, with many of these sources (large circles in Fig. 2) located between the 2 and 20 Myr isochrones. This is consistent with an independently estimated age for HD 104237 itself of around 2–3 Myr (Table 1).

From Figure 2, we identify two groups of stars for follow-up spectroscopic characterization for signs of stellar youth, such as Li I  $\lambda 6707$  absorption and enhanced optical activity:

(1) the X-ray–selected stars and (2) field stars with photometry broadly consistent with that of the *Chandra* counterparts (defined as stars with  $V$  magnitudes within  $\approx 1$  mag, for a given color, of the sequence of *Chandra* sources proximate to  $\epsilon$  Cha and HD 104237). These latter stars are indicated by the squares in Figure 2.

#### 4.2. Spectroscopic Confirmation

Optical spectroscopy of most of the *Chandra* stellar counterparts and optical photometric candidates was obtained during 2002 March and 2003 April using the 2.3 m telescope and dual-beam spectrograph (DBS) at Mount Stromlo and Siding Spring Observatories (MSSSO). Using the 1200 lines  $\text{mm}^{-1}$  grating in the red beam resulted in spectra with coverage from 6325 to 7240 Å at a 2 pixel resolution of 1.1 Å, with the slit projecting  $2''$  on the sky. For the late-type stars, exposure times of 600–3000 s yielded continuum signal-to-noise ratios of 20–100 near  $H\alpha$ . The spectra were reduced using dome flats, bias, and Fe- $\text{Ar}$  arc frames, making use of standard IRAF routines, such as *ccdproc*.

Analysis of the spectra showed that four of the *Chandra*-selected stars were active, lithium-rich late-type objects (Fig. 3). An additional T Tauri star not detected by *Chandra* was identified from the list of photometric candidates. The two optically bright *Chandra* sources in the field with proper motions discordant with  $\epsilon$  Cha and HD 104237, CPD  $-77^\circ 773$  and CPD  $-77^\circ 775$ , lack detectable Li I  $\lambda 6707$  (equivalent widths  $\text{EW} < 0.05$  Å), as do the several field stars observed with the DBS that either were detected by *Chandra* or have photometric properties similar to the  $\epsilon$  Cha–HD 104237 group stars. We did not obtain spectroscopy of three very faint *Chandra* counterparts, following the analysis of optical colors showing them not to be late-type stars.

The resulting  $H\alpha$ - and Li-region normalized spectra for  $\epsilon$  Cha, HD 104237, and the five T Tauri stars located within the *Chandra* field are shown in Figure 3, with  $H\alpha$  and Li EWs listed in Table 3. Surprisingly, for HD 104237 itself we detect Li I  $\lambda 6707$  and nearby lines, such as Ca I  $\lambda 6718$ , that are indicative of a late-type star; we discuss these spectra further in § 5.1.

#### 4.3. Rotation and Variability Studies

For several of the candidate stars identified by *Chandra* and confirmed to be PMS in our early ground-based studies, we obtained multiepoch differential photometry using the 1.0 m telescope at SAAO during 2002 April and May. Observations were made in the Cousins  $VRI$  bands for the central regions of the HD 104237 field and two distant fields containing late-type sources. For each field,  $\sim 15$  epochs were obtained over 10 nights in  $1''5$ – $3''$  conditions. The differential magnitudes for each of the T Tauri stars were determined with respect to four to six local “standard stars” within each CCD field that were found to remain constant to less than 0.01 mag. A few of the nightly data sets were also transformed to the standard system via the observation of southern photometric standard stars. Results from this study are presented in § 5.1.

### 5. THE ε CHA YOUNG STELLAR GROUP

We describe here individual stars in the  $\epsilon$  Cha field found by these X-ray and/or optical methods. The running star

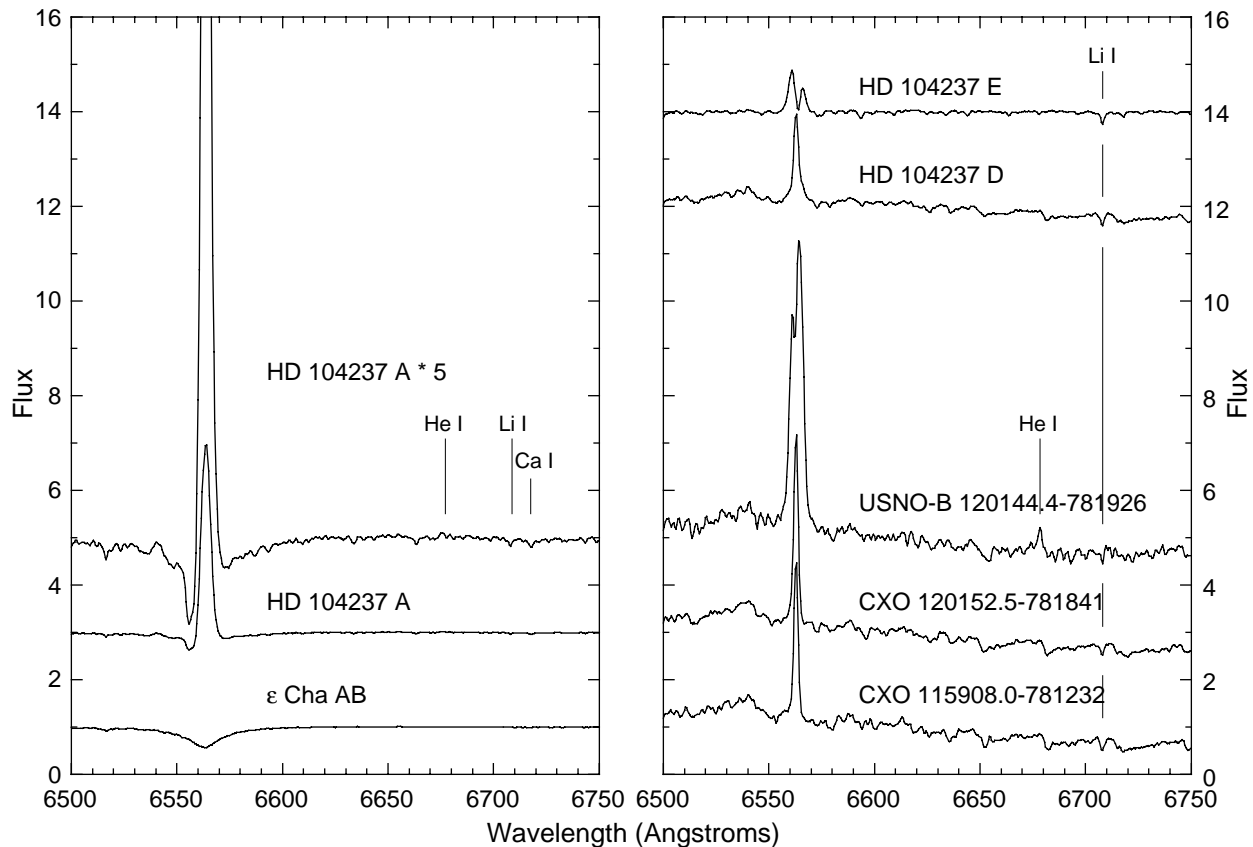


FIG. 3.—Normalized MSSSO 2.3 m/DBS spectra of  $\epsilon$  Cha group members near  $H\alpha$  and  $\text{Li I } \lambda 6707$ . The spectrum for HD 104237A is shown expanded by a factor of 5 to highlight the presence of cool-star features; see § 4.2 for details.

number, positions, names, and optical properties are given in Table 3. Column (2) summarizes whether a given star is selected as a PMS group member by virtue of its X-ray emission, its location on the PMS photometric isochrone (Fig. 2), the presence of  $H\alpha$  or  $\text{Li I } \lambda 6707$  spectroscopic indicators (Fig. 3), and/or *Hipparcos* astrometric association with  $\epsilon$  Cha–HD 104237 and the OSCA. The final column of Table 3 gives our assessment distinguishing accreting classical T Tauri (CTT) stars from nonaccreting weak-lined T Tauri (WTT) stars based on the strength and width of the  $H\alpha$  emission line.

Figure 4 shows the large-scale optical field, and Figure 5 shows the X-ray sources in the immediate vicinity of  $\epsilon$  Cha and HD 104237. X-ray spectra, variability and luminosities are given in Table 5. We give rough mass estimates based on the correlation between X-ray luminosity and mass seen in the large sample of Orion Nebula cluster stars (see Fig. 4 of Feigelson et al. 2003). Stars probably associated with  $\epsilon$  Cha and HD 104237 (confirmed members) and nonmembers are listed in separate sections of Table 3 and are described below.

### 5.1. Confirmed Members

1. *CXOU J115908.2–781232*.—Located  $\approx 2'$  west-northwest of HD 104237A, red-beam DBS spectroscopy shows that the star is of the M5 spectral type (with an uncertainty of 0.5–1 subtypes) with  $\text{EW} = -6.2 \text{ \AA}$   $H\alpha$  emission and very prominent  $\text{Li I } \lambda 6707$  absorption. Its photometric colors,  $V-R = 1.42$  and  $V-I = 3.16$ , are consistent with

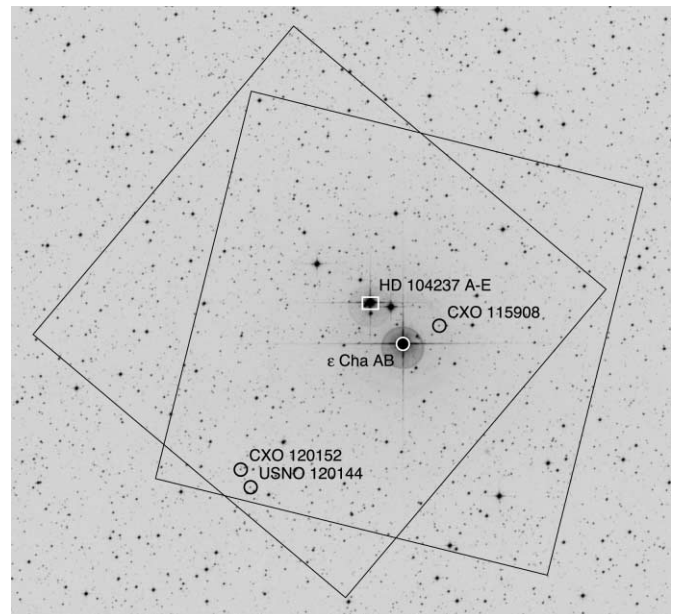


FIG. 4.—A  $26' \times 28'$  red POSS II all-sky survey image centered at  $(\alpha, \delta) = (12^{\text{h}}00^{\text{m}}30^{\text{s}}, -78^{\circ}12'00'')$  (J2000.0), overlaid with the two *Chandra* fields (Table 2). Members of the  $\epsilon$  Cha group are identified; see Table 3 for the locations and properties of these objects. The rectangle surrounding the HD 104237A–E system delineates the region of the merged *Chandra* image shown at high spatial resolution in Fig. 5.

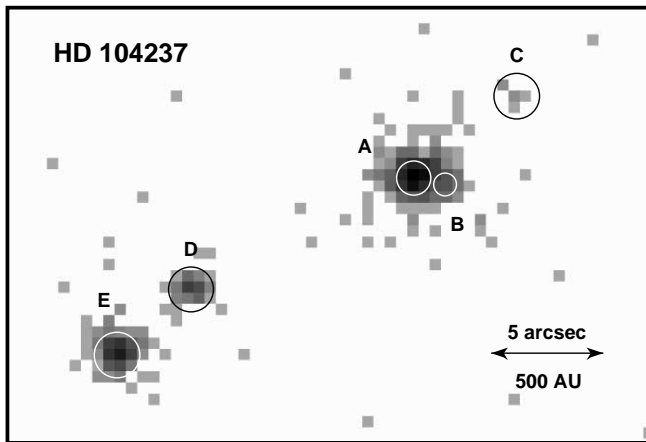


FIG. 5.—*Chandra* ACIS image in the vicinity of HD 104237. The image is displayed with  $0''.25 \times 0''.25$  pixels, and the gray scale is logarithmic, with the faintest level showing individual X-ray events. The circles show the extraction regions used in spectral analysis.

this spectral type without reddening, and its low X-ray luminosity, around  $\log L_x \simeq 28.5$  ergs  $s^{-1}$ , is typical for M-type PMS stars. The soft X-ray spectrum, with most of the counts below 1 keV, is reminiscent of the ultrasoft spectrum of the TW Hya brown dwarf TWA 5B (Tsuboi et al. 2003). Multipepoch differential *VRI* photometry obtained at SAAO during 2002 April was inconclusive; the *V*-band data were found to be variable at the  $2\sigma$  level compared to stars of similar brightness within the CCD field ( $\sigma = 0.015$  mag at  $V \approx 17$ ).

2.  $\epsilon$  Cha AB.—The star shows strong  $H\alpha$  absorption ( $EW = +13$  Å) and has photometry consistent with the established spectral type of B9 V given in the SIMBAD database. The star is a cataloged binary consisting of components with visual magnitudes of 5.4 (A) and 6.1 (B), with separation variously reported between  $0''.45$  and  $1''.9$  (ESA 1997; Worley & Douglass 1997; Dommangen & Nys 2002<sup>6</sup>). Assuming that  $\epsilon$  Cha A is spectral type B9 without significant reddening, then  $\epsilon$  Cha B is an early A star (and we adopt here A1). The projected separation of 50–200 AU implies a many centuries–long period. However, the star is a radial velocity variable on far shorter timescales, inferring a higher order of multiplicity. Buscombe (1962) lists four velocities, obtained over 120 days, that vary between  $-9$  and  $+16$  km  $s^{-1}$  and an older measurement of  $+22$  km  $s^{-1}$ . As further evidence of multiplicity, the H-R diagram placement of  $\epsilon$  Cha A (Fig. 6) suggests the star is overluminous compared to other group members (see § 5.3). The absence of any X-ray emission gives a very low limit of  $\log L_x < 27.7$  ergs  $s^{-1}$  ( $< 3$  ACIS counts). This strongly suggests that the  $\epsilon$  Cha system contains no late-type PMS companions above mid-M. This conclusion is supported by inspection of the DBS red spectrum; no late-type stellar features are evident in the  $H\alpha$  region. With its overluminosity and absence of late-type companion, we suggest that  $\epsilon$  Cha A is an unresolved binary between two BA-type stars, and thus the  $\epsilon$  Cha system in its entirety may have three BA-type stars.

3. HD 104237C.—This and the following *Chandra* source lie within  $5''$  of HD 104237A and could not be seen with the acquisition camera of the MSSSO 2.3 m in gray conditions

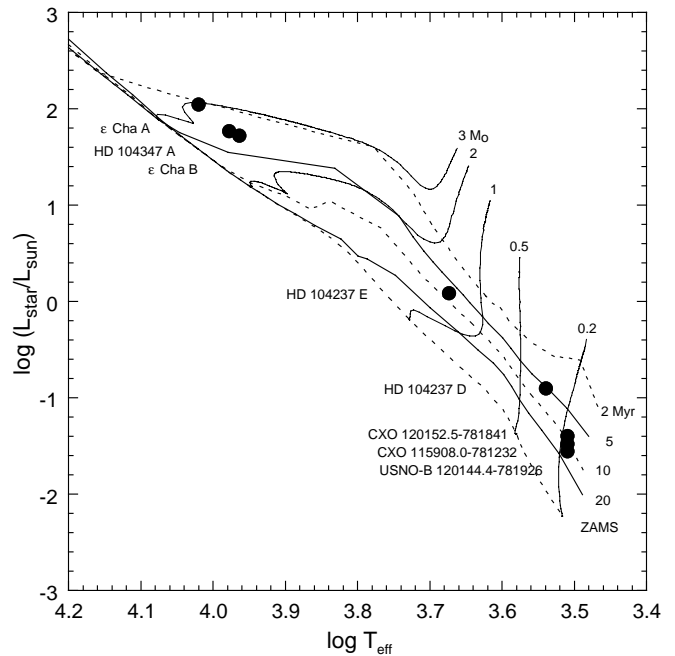


FIG. 6.—H-R diagram for the  $\epsilon$  Cha group members, identified by abbreviated names (see Table 3 for details on the individual stars). The model isochrone (in units of Myr) and isomass (in units of  $M_\odot$ ) lines are from Siess et al. (2000).

in  $\approx 2''$  seeing. They are also not listed in either the USNO-B1.0 or Two Micron All-Sky Survey (2MASS) catalogs. We therefore provide here no optical information for these sources. Component C, lying  $5''$  to the northwest, was variable in X-rays: all six of its events appeared during the second-epoch exposure. Its low X-ray luminosity is consistent with a PMS M-type star or brown dwarf.

4. HD 104237B.—Component B lies in the wings on the west side of HD 104237A's point-spread function. Its X-ray luminosity of  $\log L_x = 29.1$  ergs  $s^{-1}$  is typical of a late K or early M star. This star may be the origin of the K-type spectral features seen in HD 104237A (see below). An additional X-ray component may also be present: a weak source to the north of components A and B residing within component A's point-spread function. In this particular case, we cannot be confident of its existence or properties and do not assign it a component letter. A longer *Chandra* exposure giving sufficient signal for subarcsecond deconvolution (see, for example, the procedures in Tsuboi et al. 2003) might clearly resolve this close component.

5. HD 104237A.—Spectroscopy of the HD 104237 primary shows  $H\alpha$  in emission, as expected for an HAeBe star, with  $EW = -20$  Å. Van den Ancker et al. (1997) find  $A_V = 0.71$  mag for the star. Given the lack of absorption in most of the other  $\epsilon$  Cha members described here, we suggest that this absorption arises in the immediate environment (e.g., inflow, outflow, or disk) of this star. Surprisingly, we also detect cool-star features indicative of a K-type T Tauri star: Li I  $\lambda 6707$  and Ca I  $\lambda 6718$  are clearly detected in the expanded spectrum of Figure 3. Assuming a typical Ca I EW for K-type stars of  $0.2$ – $0.3$  Å, we find a similar EW for the Li I  $\lambda 6707$  line. The DBS spectrum was obtained along position angle (P.A.) =  $182^\circ$ , with a slit projection on the sky of  $2''$ . It seems likely that we have detected component B

<sup>6</sup> The three catalogs cited here are available at <http://vizier.u-strasbg.fr>.

(or possibly a closer component). We tentatively associate a K spectral type to component B for this reason in Table 3.

6. *HD 104237D*.—This star, 10" east-southeast of the HAeBe star, is also invisible in on-line digital sky surveys, but it was clearly distinguished with the acquisition cameras of the 1.0 m telescope at SAAO and the 2.3 m telescope at MSSSO. DBS spectroscopy indicates a spectral type of M3, with weak H $\alpha$  emission and strong Li I  $\lambda$ 6707 absorption. SAAO colors are  $V-R = 1.19$  and  $V-I = 2.66$  with uncertainties of  $\pm 0.05$  mag because of the strongly variable background from HD 104237A. The 2MASS *JHK* photometry for this star carries confusion flags because of the proximity of HD 104237A and is therefore not listed in Table 3. Within the uncertainty in the spectral type and the photometry, reddening is negligible for HD 104237D. Multiepoch *VRI* photometry from SAAO during 2002 April provides little information on the variability of the star; the nearby bright HAeBe star spoiled most of the photometric observations, which typically suffered  $\geq 2''$  seeing. However, several epochs obtained in less than 2" conditions suggested low photometric variability over the 10 day time interval of the observations. The X-ray emission also did not change between our two widely spaced observations. Its luminosity of  $\log L_x \simeq 29.3$  ergs s $^{-1}$  is consistent with that expected from an early M PMS star, and its spectrum (as with member 1) appears unusually soft.

7. *HD 104237E*.—The star is clearly resolved from HD 104237A in POSS II scans of the field. Spectroscopy obtained with the MSSSO 2.3 m telescope and both the red ( $R \approx 6000$  at H $\alpha$ ; see Fig. 3) and blue ( $R \approx 2000$  at 4500 Å) beams of the DBS spectrograph show that the star is an early K-type star. We adopt here a spectral type of K3. The red-beam spectrum shows strong Li I  $\lambda$ 6707 absorption, with  $EW = 0.5$  Å, and weak but broad H $\alpha$  with strong self-absorption. The H $\alpha$   $EW = -4.5$  Å, and it is  $\approx -6$  Å if we "correct" for the self-absorption signature. While the unabsorbed H $\alpha$   $EW$  is below the historical 10 Å separator WTT and CTT stars, it lies above the  $EW > 3$  Å boundary suggested by White & Basri (2003) for accreting K-type stars. The velocity width is  $\approx 500$  km s $^{-1}$  at the level 10% above the surrounding continuum, strongly suggestive of ongoing accretion from a circumstellar disk.

Photometry obtained at SAAO shows that the star is highly variable on a 2.45 day period, with *VRI* values at maximum light of  $V = 12.08$ ,  $V-R = 0.83$ , and  $V-I = 1.80$ . Adopting intrinsic colors (for main-sequence stars) from Kenyon & Hartmann (1995) and the extinction corrections of Bessell & Brett (1988), we find  $A_V = 1.8 \pm 0.3$  mag. (We plot the measured colors of the star in Fig. 2 and the dereddened luminosity in Fig. 6.) In this respect, HD 104237E is distinct from all the other T Tauri stars associated with  $\epsilon$  Cha and HD 104237A, which show little or no optical reddening, including the very nearby HD 104237D. Similarly, the X-ray spectrum of HD 104237E uniquely shows significant soft X-ray absorption (Table 5). The best fit gives  $\log N_H = 22.4$  cm $^{-2}$ , equivalent to  $A_V = 16$ . The star was also highly variable in X-rays with an eightfold difference between the first and second epochs. At its peak and corrected for absorption, its X-ray luminosity exceeded that of the HAeBe primary HD 104237A.

The optical reddening and X-ray absorption for this star suggest that we are viewing the surface of HD 104237E through local intervening material. While it could be associated with patchy interstellar cloud material (dust emitting

weakly at 100  $\mu$ m is seen with *IRAS* within 10' of HD 104237; Knee & Prusti 1996), we suspect that it arises from material within the stellar system. The 2MASS photometry for this star has either upper limits or confusion flags and is not listed in Table 3. A future study will detail the variability and nature of this star.

8. *USNO-B 120144.7-781926*.—The star was outside the original photometric field surveyed at SAAO during 2002 January but was found during 2002 April in a field centered on nearby CXOU J120152.8-781840.9. The star resides near the edge of the *Chandra* field but was undetected in X-rays, indicating  $\log L_x < 28.0$  ergs s $^{-1}$ . It was observed spectroscopically because it has photometric properties similar to several of the *Chandra*-selected late-type members. DBS spectroscopy obtained in 2003 April confirms that the star is an active, M5 spectral type PMS star with optical CTT star characteristics, such as strong H $\alpha$  ( $EW = -23$  Å) and He I emission at 6678 Å. Lithium is present at levels typical for T Tauri stars ( $EW = 0.6$  Å). Analysis of the optical and 2MASS photometry suggests no significant K-band excess. Multiepoch photometry obtained in 2002 April indicates that the star is highly variable, with an amplitude of  $\sim 0.2$  mag but with no detected periodicity, probably as a result of undersampling of the light curve.

9. *CXOU J120152.8-781840*.—DBS spectroscopy shows that the star is of the M5 spectral type, with moderately strong H $\alpha$  emission and Li I  $\lambda$ 6707 absorption. *VRI* photometry indicates  $V-R = 1.49$  and  $V-I = 3.26$ , consistent with the spectral type estimate. Our multiepoch photometric observations indicate no significant level of variability compared to field stars of similar magnitude. The X-ray emission was low, typical for PMS M stars, but probably variable, with 14 of 21 events arriving in the first epoch.

## 5.2. Nonmembers

*CPD -77°773*.—The H $\alpha$  line is seen weakly in absorption, and Li I  $\lambda$ 6707 is undetected, indicating that this star is not PMS. Our DBS spectroscopy and SAAO photometric color ( $V-I = 1.34$ ) are consistent with the star being an early K-type giant. SIMBAD lists a spectral type of K0.

*CPD -77°775*.—The H $\alpha$  line is strongly in absorption, and Li I  $\lambda$ 6707 is undetected, again indicating that the star is older than PMS. Our spectroscopy and color ( $V-I = 0.49$ ) indicate that the star is a (possibly mildly reddened) early F-type dwarf, supporting the SIMBAD spectral type of F0.

*CXOU J120118.2-780252*.—Located near the northern edge of the *Chandra* field, the star is a weak but highly variable X-ray source; all 17 of its photons arrived during the second *Chandra* snapshot. DBS spectroscopy shows that the star is a late K-type star, with weak H $\alpha$  emission ( $EW = -1.5$  Å) and no detection of lithium. For its spectral type, the star is  $\sim 4$  mag too faint to be associated with the  $\epsilon$  Cha PMS stellar group. If the star is main-sequence, it lies at a distance of  $\sim 250$  pc.

*Three faint Chandra counterparts*.—Optical CCD study of the faint counterparts associated with CXOU J115942.2-781836, CXOU J120101.4-780618, and CXOU J120135.3-780427 shows that none have photometric properties consistent with late-M stars or brown dwarfs associated with  $\epsilon$  Cha and HD 104237. *VRI* photometry obtained for these objects at SAAO during 2003 April indicates colors consistent with early K-type dwarfs. None of these

objects were observed with the DBS spectrograph. If main-sequence K stars, they must lie at distances of 2–4 kpc, inferring an unrealistically high  $\log L_t > 30$  ergs s<sup>-1</sup>. If instead these objects are active galaxies, they are unresolved at the  $\approx 1''.5$  resolution of the SAAO CCD images.

*Three additional photometric candidates.*—The final three stars in Table 3 have  $V$  magnitudes that, for their  $V-I$  color, fell within  $\approx 1$  mag (fainter) of the sequence of *Chandra*-detected late-type stars in the  $\epsilon$  Cha–HD 104237 field. We observed them with the DBS spectrograph and found two early K and one early M star. None were active, lithium-rich objects; all are likely field giants.

### 5.3. An H-R Diagram for the $\epsilon$ Cha Group

Based on these photometric and spectroscopic characterizations of the PMS stars associated with  $\epsilon$  Cha and HD 104237, we produce in Figure 6 an H-R diagram of group members. The spectral type– $T_{\text{eff}}$  and bolometric correction sequences for main-sequence stars given by Kenyon & Hartmann (1995) are used. Locations of the  $\epsilon$  Cha group stars are compared to the PMS evolutionary grids of Siess et al. (2000), from which several isochrone and isomass lines are shown.

We find that the HAeBe star HD 104237A and  $\epsilon$  Cha B lie near the 3 Myr isochrone, and the two well-characterized companions to HD 104237A, HD 104237D and HD 104237E, lie near the 5 Myr isochrone. Since *Chandra* imaging and DBS optical spectroscopy for HD 104237A show evidence for one (or maybe two) very nearby late-type companions, its position in the H-R diagram is likely slightly elevated. It is also dependent on the quality of the reddening estimate ( $A_V = 0.71$  mag) given by van den Ancker et al. (1997), which we have applied to HD 104237A.<sup>7</sup>

In Figure 6, we show  $\epsilon$  Cha AB as a B9+A1 system, with a 0.7 mag brightness difference. As noted in § 5.1,  $\epsilon$  Cha A appears to be elevated in luminosity (and therefore appears younger) compared to the isochronal locus of  $\epsilon$  Cha B, HD 104237A, HD 104237D, and HD 104237E. The discrepant position of  $\epsilon$  Cha A may be grid-dependent or, as discussed in § 5.1, it is a close binary itself with detected radial velocity variations. We thus suspect that  $\epsilon$  Cha A consists of two components, which fall near the 3–5 Myr isochrones.

The three active, lithium-rich M5 stars (CXOU J115908.2–781232, USNO-B 120144.7–781926, and CXOU J120152.8–781840) appear systematically older than the stars of earlier spectral type. Their H-R diagram placement implies an age of  $\sim 10$  Myr. In considering the ages of these stars compared to other group members, we discuss two possibilities:

1. The star-grid comparison may be flawed for late M stars. Here comparison with the  $\sim 9$  Myr old  $\eta$  Cha cluster stars is valuable. Lawson & Feigelson (2001) found that the grids of Siess et al. (2000) best achieved coevality across the

<sup>7</sup> Our 3–5 Myr estimate for  $\epsilon$  Cha B and the HD 104237A–E system using Siess et al. (2000) tracks can be compared to the 2 Myr estimate given by van den Ancker et al. (1997) for HD 104237A, using Palla & Stahler (1993) tracks. Along with the observational considerations discussed above, the age difference is also likely model-dependent. Comparing several sets of PMS evolutionary grids to the H-R diagram location of members of the  $\sim 9$  Myr old  $\eta$  Cha cluster, Lawson & Feigelson (2001) found that the more recent Palla & Stahler (1999) models gave factor of  $\sim 2$  younger inferred ages for early-type stars compared to the Siess et al. (2000) models.

then-known  $\eta$  Cha cluster population ranging from spectral type B8 to M3. Since then, ongoing study of the cluster stellar population has discovered several M4–M5 stars residing less than 20' from the cluster center that appear older than earlier type cluster members when compared to Siess et al. (2000) tracks (Lyo et al. 2003a). In the  $\eta$  Cha cluster, the age discrepancy appears rapidly for stars with  $V-I > 3$ ; i.e., for stars later than  $\approx$ M3 (or  $T_{\text{eff}} < 3400$  K). The same phenomenon appears in the late-type  $\epsilon$  Cha stars. We suggest a variety of possible causes: a deficient temperature calibration, in either the models or the application of the Kenyon & Hartmann (1995) main-sequence temperature calibration to PMS stars; an incorrect treatment of the stellar luminosities, perhaps due to the large bolometric corrections required to transform the observations; or theoretical errors in the treatment of opacities in the M star models.

2. It is likely that the rich,  $\approx 15$  Myr old OSCA subgroups have evaporated members into the Chamaeleon vicinity (Blaauw 1991; de Geus 1992). If we make the hypothetical and optimistic assumption that half of the subgroup members have dispersed into a halo across the region of the sky shown in Figure 1, then a typical *Chandra* ACIS observation will contain on average only  $\sim 0.04$  OSCA PMS stars. This explanation is clearly inadequate to explain three M stars in the  $\epsilon$  Cha–HD 104237 ACIS field. We conclude that these three stars are probably  $\epsilon$  Cha group members and thus coeval with the higher mass members.

In summary, the  $\epsilon$  Cha PMS stellar group currently consists of  $\epsilon$  Cha, with two confirmed, and quite possibly a third, late B/early A stars within  $\approx 200$  AU; HD 104237, with an A star and four confirmed (and possibly a fifth) late-type companions within  $\approx 1500$  AU; and three mid-M stars distributed over  $\approx 0.5$  pc. Our best estimate for the group age is 3–5 Myr.

## 6. PMS STARS AROUND THE OTHER HAeBe STARS

Figure 7 and Table 5 summarize the X-ray results within 1000 AU of the four other HAeBe targets, and Table 4 gives X-ray sources likely associated with stars in the full ACIS fields. We have not made any optical study of these fields.

Table 4 shows that three of the four HAeBe stars each have several likely stellar X-ray sources dispersed in the ACIS fields, i.e., with projected distances more than 1000 AU and less than 0.3 pc from the targeted HAeBe star. HD 141569 is the exception, with no additional stellar X-ray sources. This is easily interpretable by reference to their global positions with respect to the OSCA shown in Figure 1: HD 100546, HD 150193, and HD 152404 lie within the traditional boundaries of the rich OSCA subgroups, while HD 141569 does not. These new X-ray stars are thus likely members of the OSCA, and we suspect that they are not dynamically linked to the HAeBe stars.

Details on these proposed OSCA X-ray stars are given in Table 4 and its notes. They include several unstudied late-type stars with  $K \approx 11$  around HD 100546 in the LCC subgroup; the CTT star CXOU J163945.5–240202 = IRAS 16367–2356 in the Oph cloud complex; the late-type star CXOU J164031.3–234915 and its (probably) intermediate-mass companion, also in the Oph cloud complex; and CXOU J165430.7–364924 = HD 152368 (B9 V) and a probable late-type companion in the UCL subgroup.

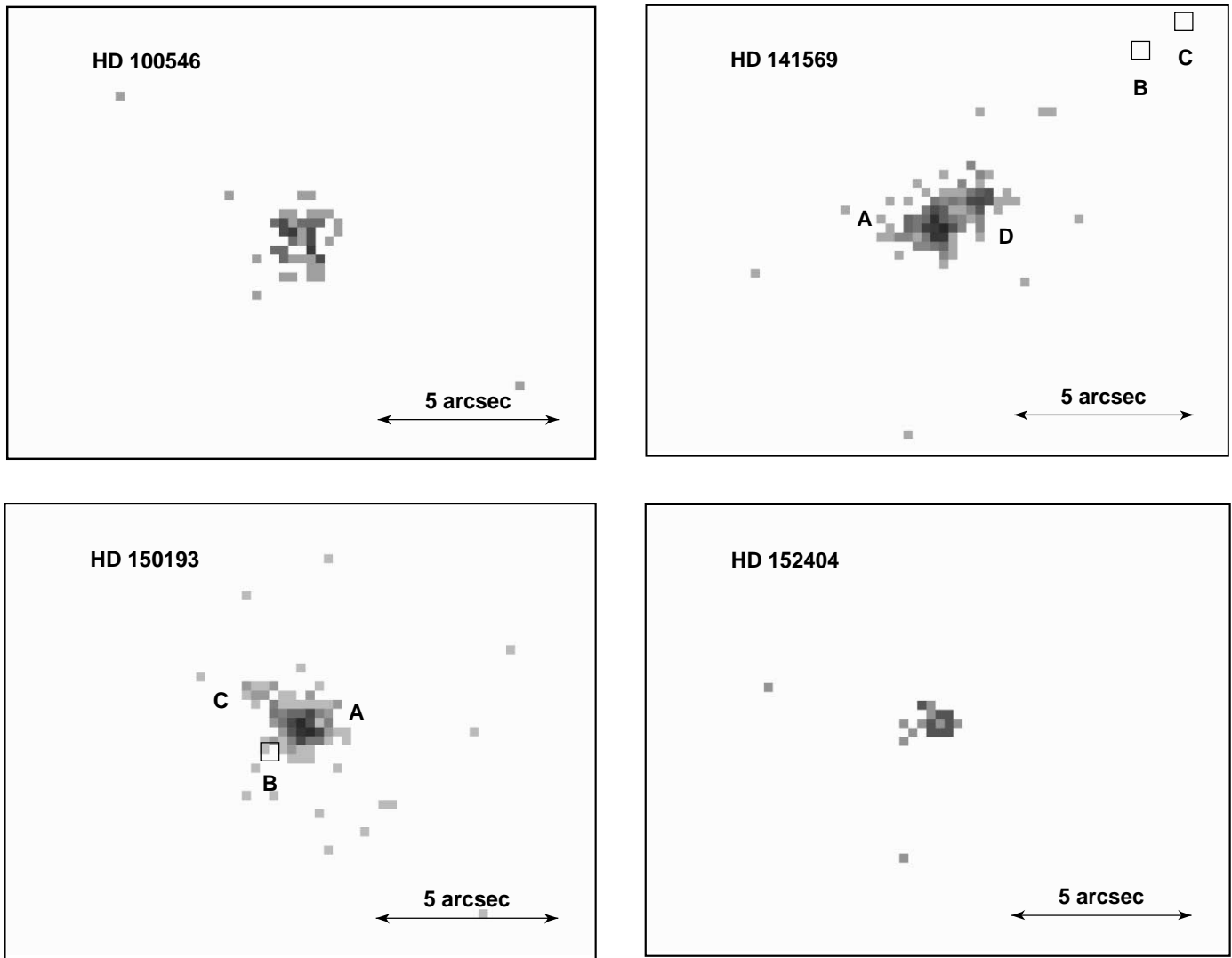


FIG. 7.—*Chandra* ACIS image in the vicinity of four H AeBe objects. The image is displayed with  $0''.25 \times 0''.25$  pixels, and the gray scale is logarithmic, with the faintest level showing individual X-ray events. The boxes indicate companions found at optical and infrared wavelengths.

Stars in the immediate vicinity of the H AeBe targets are as follows. Recall that we have made  $\approx 1''$  alignments of the *Chandra* images, assuming that the brightest source is coincident with the primary, which may not always be correct.

**HD 100546.**—The *Chandra* image shows a single source with modest emission around  $2 \times 10^{29}$  ergs  $s^{-1}$ , typical of PMS K stars (Feigelson et al. 2003). The photon distribution appears slightly extended from the usual point-spread function, but any multiplicity must lie within  $1''$  of the primary.<sup>8</sup> Several non-X-ray-emitting stars lie within  $10''$  of the primary, but these are most likely background stars unrelated to the H AeBe star (Grady et al. 2001).

**HD 141569.**—This system is clearly resolved into two components separated by  $1''.5$  along P.A. =  $300^\circ$ , where the secondary to the northwest is only slightly fainter than the primary.<sup>9</sup> The projected separation is 150 AU. We call this

<sup>8</sup> The disk of HD 100546 is seen in scattered light out to  $4''$  and in millimeter emission out to  $\sim 30''$ , extended in the southeast-northwest direction (Clampin et al. 2003; Henning et al. 1998).

<sup>9</sup> There is a hint of a third component  $0''.7$  from the primary along P.A. =  $90^\circ$ , with around 10 photons, but it cannot be clearly discriminated from the wings of the primary point-spread function.

component “D” because two other companions, “B” and “C,” established to share the primary’s proper motion, have been found in optical images (Weinberger et al. 2000). From their H-R diagram locations, the estimated masses of components B and C are  $0.45$  and  $0.22 M_\odot$ , respectively, with an age of 3 Myr. The high X-ray luminosity of HD 141569D,  $\log L_x \approx 29.9$  ergs  $s^{-1}$ , suggests a mass of around  $1 M_\odot$ . The absence of components B and C from the *Chandra* image is not surprising, as a large fraction of the Orion Nebula M-type stars fall below the  $\log L_x \approx 28.0$  ergs  $s^{-1}$  sensitivity limit of the brief exposure available here (Feigelson et al. 2003).

**HD 150193.**—This source is also double, with a component “C” lying  $1''.5$  from the primary along P.A. =  $55^\circ$ . The projected separation is 220 AU. Although its X-ray emission is 5–10 times fainter than that of the primary, the luminosity is still consistent with a  $\approx 1 M_\odot$  PMS star. The *Chandra* image does not show component “B” (unknown spectral type)  $1''.1$  to the southwest of the primary, reported from *K*-band imagery (Pirzkal, Spillar, & Dyck 1997).

**HD 152404.**—This source is weak and unresolved in the *Chandra* image. It is a double-lined spectroscopic binary with period 13.6 days and eccentricity 0.47 (Andersen et al.

1989). The spectral type is F5 IVe, and the components have equal masses around  $1.5 M_{\odot}$ .

## 7. DISCUSSION AND CONCLUDING REMARKS

### 7.1. *The Multiplicity and X-Ray Emission of HAeBe Stars*

*Chandra* imagery is clearly a useful complement to high-resolution optical and near-infrared imagery and spectroscopy in the study of the multiplicity (i.e., companions within  $\approx 1000$  AU) of intermediate-mass PMS stars. In the X-ray band, the primary is not orders of magnitude brighter than the companions, so coronagraphic methods are not necessary. Combining the results of §§ 5 and 6 with optical-infrared studies, we find a quintet (or possibly sextet) in HD 104237, a quartet in HD 141569, a triple in HD 150193, a double in HD 100546, and a single in HD 152404. Half of these companions were discovered in the *Chandra* images. If the primary's X-ray emission arises from an unresolved lower mass companion (see below), then the multiplicity of each star is increased by at least one. *Chandra* imagery is limited in two respects: it detects only a fraction of PMS M-type and brown dwarfs (although it should be nearly complete for higher mass stars if sensitivities reach  $\log L_t \approx 28.0$  ergs  $s^{-1}$ ; Feigelson et al. 2003); and it cannot resolve companions closer than  $\approx 1''$  from the primary.

The X-ray emission from intermediate-mass HAeBe stars, and AB stars in general, has been a long-standing puzzle, as stars without outer convection zones should not have a magnetic dynamo of the type known in lower mass stars. Recent *Chandra* images of nearby main-sequence B stars have confirmed that, in at least four of five cases, the emission arises from late-type companions (Stelzer et al. 2003). For HAeBe stars, it has been debated whether the X-rays are from companions or are produced by the primary through star-disk magnetic interaction (Zinnecker & Preibisch 1994; Skinner & Yamauchi 1996).

Our results do not clearly solve this puzzle. The five primary HAeBe stars observed here have X-ray luminosities in the range  $29.1 \text{ ergs s}^{-1} < \log L_X < 30.7 \text{ ergs s}^{-1}$  in the 0.5–8 keV band, with plasma energies in the range  $0.4 \text{ keV} < kT < 5 \text{ keV}$ . These properties are consistent with intermediate-mass Orion Nebula cluster A- and B-type stars, most of which are probably not actively accreting, as well as solar-mass PMS stars (Feigelson et al. 2002). Our *Chandra* images show that some of the X-rays attributed to HAeBe stars from low-resolution *ROSAT* and *ASCA* studies are produced by resolved stellar companions, but most of the emission still arises from within  $1''$  of the primary. This could be either a close, unresolved companion or the accreting primary itself. In the former case, the companion must have  $\gtrsim 1 M_{\odot}$  because substantially lower mass stars are fainter with X-ray luminosities in the  $\log L_X < 28$ – $29$  ergs  $s^{-1}$  range (Feigelson et al. 2003). In the latter case, the mechanism of HAeBe X-ray production must give X-ray properties essentially indistinguishable from those of solar-mass PMS stars.

### 7.2. *HD 104237 as a Bound, High-Multiplicity Stellar System*

At least a quintet, HD 104237 is the highest multiplicity HAeBe star known. The majority of HAeBe stars lie in binaries (Leinert, Richichi, & Haas 1997; Pirzkal et al. 1997;

Corporon & Lagrange 1999), and a few are in triple systems (TY CrA: Casey et al. 1995; NX Pup: Brandner et al. 1995). Several quartets of lower mass PMS stars have been found, including GG Tau, UZ Tau, UX Tau, V773 Tau, HD 98800, and BD +26°718B. It is very unlikely that any of the companions HD 104237B–E seen in the *Chandra* image appear projected so close to the primary by chance:  $P \approx 1\%$  for a randomly located PMS star or (for components B and C, without optical spectroscopic confirmation)  $P \approx 0.1\%$  for a randomly located extragalactic X-ray source.

The system must be bound. If the stars were formed independently with the  $\approx 0.5 \text{ km s}^{-1}$  velocity dispersion characteristic of small molecular clouds (Efremov & Elmegreen 1998), it would disperse within a few thousand years. Unlike many other multiple systems (such as HD 98800, GG Tau, and Castor), the HD 104237 components do not exhibit a hierarchical orbital structure of two or three close binary pairs. Because of the fragility of its orbits, we can infer that the HD 104237 system as a whole has not been ejected from some larger stellar aggregate but rather was born in a dynamically quiescent environment (Kroupa 1998).

Perhaps of greatest interest, the HD 104237 quintet has apparently not suffered from serious internal dynamical instabilities during the  $10^2$ – $10^3$  orbits of its 3–5 Myr lifetime. Instabilities leading to ejection of some members are thought to be common in multiple-PMS-star systems (e.g., Sterzik & Durisen 1995, 1998; Reipurth 2000). In their dynamical calculations of stellar systems with realistic mass distributions, Sterzik & Durisen (1998) find that 98% of quintuple systems with an intermediate-mass primary will eject two or more members within 300 orbits. Also, the disks of at least two of its constituent stars—HD 104237A and HD 104237E—have not been destroyed, as expected from close dynamical encounters (Armitage & Clarke 1997). HD 104237 thus appears to be an unusually stable high-multiplicity system, probably born under quiescent conditions in the low-density environment of a small molecular cloud.

### 7.3. *Large-scale Environment of the $\epsilon$ Cha Group*

On a  $\sim 10^\circ$  scale, the interstellar environment is relatively free of molecular material between the Cha I and Cha II clouds, which have 1000 and 1900  $M_{\odot}$  of molecular gas and lie at distances of 160 and 180 pc, respectively (Mizuno et al. 2001). The  $\epsilon$  Cha group lies in front of a dusty screen that covers the entire Chamaeleon-Musca region at a distance of 150 pc (Franco 1991; Knude & Hog 1998). On a smaller ( $10'$ ) scale, three small clumps of CO and far-infrared emission are found between and west of  $\epsilon$  Cha and HD 104237 (Knee & Prusti 1996). These cloudlets are probably translucent, with masses below  $0.5 M_{\odot}$ .

Recent studies report young stars on large scales that may be associated with the compact  $\epsilon$  Cha group discussed here. Sartori, Lépine, & Dias (2003) place  $\epsilon$  Cha and HD 104237 on the near edge of a proposed new Chamaeleon OB association, with 21 identified B- and A-type stars spread over  $\sim 10^\circ$ – $20^\circ$  (50–100 pc). This new grouping appears as a nearly continuous extension of the well-known US, UCL, and LCC OSCA subgroups. Mamajek (2003) criticizes this finding on the grounds that there is no overdensity of B stars in this region and the derived velocity dispersion is consistent with random field stars. Blaauw (1991) had earlier suggested an extension of the LCC subgroup B stars into the

Carina-Volans region next to Chamaeleon. From an extensive spectroscopic survey of later type southern stars, Quast et al. (2003) define a stellar association called “ $\epsilon$  Cha A,” with at least 15 K-type members spanning  $10^\circ$ – $15^\circ$  in Chamaeleon. These stars are lithium-rich, with ages around 10 Myr. Here again, it is difficult to distinguish between members of the proposed new grouping and an extended or evaporating LCC subgroup. Frink et al. (1998) previously reported seven comoving T Tauri stars over a subregion of this association around  $\epsilon$  Cha, but with different kinematic properties.

We do not derive a clear view of the large-scale young stellar environment of  $\epsilon$  Cha from these confusing reports. Many young stars are present, but it is difficult or impossible to distinguish distinct clusters from the profusion of outlying and evaporated stars likely to surround the rich Oph, US, UCL, and LCC OSCA concentrations. For the brighter B- and A-type stars, it is also difficult to distinguish 5–20 Myr stars physically associated with the OSCA from somewhat older field stars unless late-type companions can be found and characterized.

#### 7.4. Origin of the $\epsilon$ Cha Group

The link between the brightest members  $\epsilon$  Cha and HD 104237 as comoving, likely coeval PMS stars has been repeatedly discussed in the past (Hu et al. 1991; Knee & Prusti 1996; Shen & Hu 1999; Mamajek et al. 2000). But there has been debate regarding their origin. Writing before the *Hipparcos* parallax measurement of 114 pc was available for the group, Knee & Prusti (1996) suggested that the system lies around 140 pc away and that the nearby interstellar cloudlets were part of the Cha II star-forming region. Writing after the release of *Hipparcos* measurements, Eggen (1998) showed that the system is more likely a member of the Local Association (which includes the OSCA), although he did not list it as an OSCA member. We establish (Mamajek et al. 2000 and Table 1) that the extrapolated motions of HD 104237 and  $\epsilon$  Cha lie within 10 pc of (within measurement errors, consistent with exact coincidence with) the centroid of OSCA subgroups in the past  $\sim 10$  Myr.

We believe that this kinematic link between the  $\epsilon$  Cha group and the OSCA is reasonably convincing evidence that they originated in the same GMC. The question then arises why HD 104237 is judged from its H-R diagram location to have an age far younger than the nearest OSCA subgroup: based on isochrones in the H-R diagram, we find an age of 3–5 Myr for the  $\epsilon$  Cha group (§ 5.3), while the UCL subgroup has age of 17 Myr (Mamajek et al. 2002). The same question can be raised about the  $\eta$  Cha cluster, which, with an age no older than 9 Myr (Lawson et al. 2001; Lawson & Feigelson 2001), is younger than the nearest OSCA subgroup, the LCC, with an age of 16 Myr.

Such age discrepancies can be explained within the dispersal scenario outlined by Feigelson (1996). The scenario is based on the dispersion of different portions of a GMC along velocity vectors established by turbulence processes. Some portions of the cloud complex form rich stellar clusters relatively early and dissipate their molecular material soon afterward (Kroupa 2000). Other portions of the complex remain as gaseous clouds as they disperse, forming stars at different times and far from the OB-rich environments of the larger clusters. This corresponds to the super-virial cloudlet regime, where  $Q = \|\text{kinetic energy}/$

gravitational energy  $\| > 1$  and cloudlets fly apart without collisions, described in the recent hydrodynamic study by Gittins, Clarke, & Bate (2003). Thus, relatively young, sparse groups, such as those around  $\eta$  Cha and  $\epsilon$  Cha, may be found in the vicinity of older clusters like the OSCA subgroups. Some of these dispersed groups may be compact (like the  $\eta$  Cha and  $\epsilon$  Cha groups) because of smaller local values of  $Q$ , while other groups with higher  $Q$  may themselves appear widely dispersed (like the TW Hya association and  $\beta$  Pic moving group; see § 2 and Fig. 1). However, all of these systems would share space motions converging onto the same ancestral GMC.

#### 7.5. Comparison of the $\eta$ Cha and $\epsilon$ Cha Groups

We have now made considerable progress in characterizing the populations of two nearby sparse PMS stellar clusters dominated by intermediate-mass stars and lying on the outskirts of a large and rich OB association:

1. The  $\eta$  Cha cluster has three intermediate-mass systems: the B8 star  $\eta$  Cha, probably (because of its *ROSAT* X-ray detection) with a low-mass companion; RS Cha, an A7+A8 hard binary with a likely lower mass companion; and the single A1 star HD 75505 (Mamajek et al. 2000). These three systems have projected separations  $\leq 0.25$  pc. They are accompanied by 14 late-type primaries, of which several are binaries (Lyo et al. 2003a). Disks are pervasive in the cluster: two of the intermediate-mass systems ( $\eta$  Cha and HD 75505) have weak  $L$ -band excesses;  $\simeq 4$  of the late-type members have both IR excesses and optical signatures of active accretion; and  $\simeq 3$  additional late-type members have weak  $L$ -band excesses (Lawson et al. 2002; Lyo et al. 2003b).

2. The  $\epsilon$  Cha group has two intermediate-mass systems:  $\epsilon$  Cha, with two or three  $\sim$ A0 stars; and HD 104237, with at least four lower mass companions. Because of the absence of X-ray emission, we infer that  $\epsilon$  Cha does not have any lower mass companions above  $M \simeq 0.3 M_\odot$ . These high-multiplicity systems have a projected separation of 0.07 pc. The group also has three M5 stars distributed over 0.5 pc. Three members—HD 104237A, HD 104237E, and USNO-B 120144.4–782936—have CTT-type optical emission lines, indicating active accretion. This group has not been surveyed in the  $L$  band like  $\eta$  Cha, so the apparent lower disk fraction may not be real.

These stellar systems are quite similar, and together they paint a portrait of  $N \sim 10$ – $100$  member groups several million years after their formation. In each group, the total stellar mass is about 15–20  $M_\odot$ , and the size is  $r \approx 0.5$  pc, giving an escape velocity of  $\sim 0.5$  km s $^{-1}$ . As this is about the expected velocity dispersion inherited from the molecular material (§ 7.2), the outlying members of the groups could be unbound. It is likely that the original census was considerably higher and that many members of the original clusters have already escaped into the stellar field. The survival of so many high-multiplicity systems and disks in these sparse groups implies that little or no close dynamical interactions have occurred among the stars.

We thank A.-R. Lyo (UNSW@ADFA) for her very capable assistance with the optical spectroscopy, and L. Crause (Cape Town) for her expert reduction of the optical

photometry. J. Skuljan (Canterbury) and E. Mamajek (Arizona) provided helpful assistance with kinematical calculations, and P. Broos and L. Townsley (Penn State) developed critical *Chandra* data analysis tools. E. Mamajek (Arizona), C. Torres (LNA Brazil), and an anonymous referee suggested helpful improvements to the manuscript. We thank the SAAO and MSSSO telescope allocation

committees for observing time, and E. D. F. appreciates the University of New South Wales and Australian Defence Force Academy for hospitality during much of this work. We greatly benefitted from the SIMBAD, 2MASS, and USNO databases. This study was supported by NASA contract NAS8-38252 (PI: G. P. G.) and UNSW@ADFA URSP, FRG, and SRG research grants (PI: W. A. L.).

## REFERENCES

- Adams, F. C., & Myers, P. C. 2001, *ApJ*, 553, 744  
 Andersen, J., Lindgren, H., Hazen, M. L., & Mayor, M. 1989, *A&A*, 219, 142  
 Armitage, P. J., & Clarke, C. J. 1997, *MNRAS*, 285, 540  
 Aspin, C., & Barsony, M. 1994, *A&A*, 288, 849  
 Barbier-Brossat, M., & Figon, P. 2000, *A&AS*, 142, 217  
 Bessell, M. S., & Brett, J. M. 1988, *PASP*, 100, 1134  
 Blaauw, A. 1964, *ARA&A*, 2, 213  
 ———. 1991, in *The Physics of Star Formation and Early Stellar Evolution*, ed. C. J. Lada & N. D. Kylafis (NATO ASI Ser. C, 342; Dordrecht: Kluwer), 125  
 Bodenheimer, P., Burkert, A., Klein, R. I., & Boss, A. P. 2000, in *Protostars and Planets IV*, ed. V. Mannings, A. P. Boss, & S. S. Russell (Tucson: Univ. Arizona Press), 675  
 Bonnell, I. A. 2000, in *ASP Conf. Ser. 198, Stellar Clusters and Associations: Convection, Rotation, and Dynamos*, ed. R. Pallavicini, G. Micela, & S. Sciortino (San Francisco: ASP), 161  
 Bonnell, I. A., & Clarke, C. J. 1999, *MNRAS*, 309, 461  
 Boss, A. P. 2002, *ApJ*, 568, 743  
 Brandner, W., Bouvier, J., Grebel, E. K., Tessier, E., de Winter, D., & Beuzit, J.-L. 1995, *A&A*, 298, 818  
 Brandner, W., & Köhler, R. 1998, *ApJ*, 499, L79  
 Buscombe, W. 1962, *MNRAS*, 124, 189  
 Casey, B. W., Mathieu, R. D., Suntzeff, N. B., & Walter, F. M. 1995, *AJ*, 109, 2156  
 Clampin, M., et al. 2003, *AJ*, 126, 385  
 Clarke, C. J., Bonnell, I. A., & Hillenbrand, L. A. 2000, in *Protostars and Planets IV*, ed. V. Mannings, A. P. Boss, & S. S. Russell (Tucson: Univ. Arizona Press), 151  
 Corporon, P., & Lagrange, A.-M. 1999, *A&AS*, 136, 429  
 de Geus, E. J. 1992, *A&A*, 262, 258  
 de Zeeuw, P. T., Hoogerwerf, R., de Bruijne, J. H. J., Brown, A. G. A., & Blaauw, A. 1999, *AJ*, 117, 354  
 Dommanget, J., & Nys, O. 2002, *Observations et Travaux*, 54, 5  
 Duquennoy, A., & Mayor, M. 1991, *A&A*, 248, 485  
 Efremov, Y. N., & Elmegreen, B. G. 1998, *MNRAS*, 299, 588  
 Eggen, O. J. 1998, *AJ*, 116, 1314  
 Elmegreen, B. G., Efremov, Y., Pudritz, R. E., & Zinnecker, H. 2000, in *Protostars and Planets IV*, ed. V. Mannings, A. P. Boss, & S. S. Russell (Tucson: Univ. Arizona Press), 179  
 Elmegreen, B. G., & Lada, C. J. 1977, *ApJ*, 214, 725  
 ESA 1997, *The Hipparcos and Tycho Catalogues*, ed. M. A. C. Perryman (ESA SP-1200; Noordwijk: ESA)  
 Feigelson, E. D. 1996, *ApJ*, 468, 306  
 Feigelson, E. D., Broos, P., Gaffney, J. A., III, Garmire, G., Hillenbrand, L. A., Pravdo, S. H., Townsley, L., & Tsuboi, Y. 2002, *ApJ*, 574, 258  
 Feigelson, E. D., Gaffney, J. A., III, Garmire, G., Hillenbrand, L. A., & Townsley, L. 2003, *ApJ*, 584, 911  
 Feigelson, E. D., & Montmerle, T. 1999, *ARA&A*, 37, 363  
 Franco, G. A. P. 1991, *A&A*, 251, 581  
 Freeman, P. E., Kashyap, V., Rosner, R., & Lamb, D. Q. 2002, *ApJS*, 138, 185  
 Frink, S., Röser, S., Alcalá, J. M., Covino, E., & Brandner, W. 1998, *A&A*, 338, 442  
 Gittins, D. M., Clarke, C. J., & Bate, M. R. 2003, *MNRAS*, 340, 841  
 Grady, C. A., et al. 2001, *AJ*, 122, 3396  
 Henning, T., Burkert, A., Launhardt, R., Leinert, C., & Stecklum, B. 1998, *A&A*, 336, 565  
 Hillenbrand, L. A., Meyer, M. R., Strom, S. E., & Skrutskie, M. F. 1995, *AJ*, 109, 280  
 Hoogerwerf, R., & Aguilar, L. A. 1999, *MNRAS*, 306, 394  
 Hu, J. Y., Blondel, P. F. C., Catala, C., Talavera, A., Thé, P. S., Tjin A Djie, H. R. E., & de Winter, D. 1991, *A&A*, 248, 150  
 Kaastra, J. S., & Mewe, R. 2000, in *Atomic Data Needs for X-Ray Astronomy*, ed. M. A. Bautista, T. R. Kallman, & A. K. Pradhan (NASA CP-2000-209968; Greenbelt: NASA), 161  
 Kenyon, S. J., & Hartmann, L. 1995, *ApJS*, 101, 117  
 Klessen, R. S. 2001, *ApJ*, 556, 837  
 Knee, L. B. G., & Prusti, T. 1996, *A&A*, 312, 455  
 Knude, J., & Hog, E. 1998, *A&A*, 338, 897  
 Kroupa, P. 1998, *MNRAS*, 298, 231  
 Kroupa, P. 2000, in *ASP Conf. Ser. 211, Massive Stellar Clusters*, ed. A. Lançon & C. M. Boily (San Francisco: ASP), 233  
 Kroupa, P., & Boily, C. M. 2002, *MNRAS*, 336, 1188  
 Larson, R. B. 2002, *MNRAS*, 332, 155  
 Lawson, W. A., Crause, L. A., Mamajek, E. E., & Feigelson, E. D. 2001, *MNRAS*, 321, 57  
 ———. 2002, *MNRAS*, 329, L29  
 Lawson, W., & Feigelson, E. D. 2001, in *ASP Conf. Ser. 243, From Darkness to Light: Origin and Evolution of Young Stellar Clusters*, ed. T. Montmerle & P. André (San Francisco: ASP), 591  
 Leinert, C., Richichi, A., & Haas, M. 1997, *A&A*, 318, 472  
 Loren, R. B. 1989, *ApJ*, 338, 902  
 Lyo, A.-R., Lawson, W. A., Feigelson, E. D., & Crause, L. A. 2003a, *MNRAS*, in press  
 Lyo, A.-R., Lawson, W. A., Mamajek, E. E., Feigelson, E. D., Sung, E.-C., & Crause, L. A. 2003b, *MNRAS*, 338, 616  
 Mamajek, E. E. 2003, in *Open Issues in Local Star Formation and Early Stellar Evolution*, ed. J. Gregorio-Hetem & J. Lépine (Dordrecht: Kluwer)  
 Mamajek, E. E., & Feigelson, E. D. 2001, in *ASP Conf. Ser. 244, Young Stars Near Earth: Progress and Prospects*, ed. R. Jayawardhana & T. Greene (San Francisco: ASP), 104  
 Mamajek, E. E., Lawson, W. A., & Feigelson, E. D. 1999, *ApJ*, 516, L77  
 ———. 2000, *ApJ*, 544, 356  
 Mamajek, E. E., Meyer, M. R., & Liebert, J. 2002, *AJ*, 124, 1670  
 Mathieu, R. D. 1994, *ARA&A*, 32, 465  
 Mizuno, A., Yamaguchi, R., Tachihara, K., Toyoda, S., Aoyama, H., Yamamoto, H., Onishi, T., & Fukui, Y. 2001, *PASJ*, 53, 1071  
 Mizuno, A., et al. 1998, *ApJ*, 507, L83  
 Monet, D. G., et al. 2003, *AJ*, 125, 984  
 Ortega, V. G., de la Reza, R., Jilinski, E., & Bazzanella, B. 2002, *ApJ*, 575, L75  
 Palla, F., & Stahler, S. W. 1993, *ApJ*, 418, 414  
 ———. 1999, *ApJ*, 525, 772  
 Pirzkal, N., Spillar, E. J., & Dyck, H. M. 1997, *ApJ*, 481, 392  
 Preibisch, T., Balega, Y., Hofmann, K.-H., Weigelt, G., & Zinnecker, H. 1999, *NewA*, 4, 531  
 Preibisch, T., Brown, A. G. A., Bridges, T., Guenther, E., & Zinnecker, H. 2002, *AJ*, 124, 404  
 Quast, G. R., Torres, C. A. O., Melo, C. H. F., Sterzik, M., de la Reza, R., & da Silva, L. 2003, in *Open Issues in Local Star Formation and Early Stellar Evolution*, ed. J. Gregorio-Hetem & J. Lépine (Dordrecht: Kluwer)  
 Reipurth, B. 2000, *AJ*, 120, 3177  
 Sartori, M. J., Lépine, J. R. D., & Dias, W. S. 2003, *A&A*, 404, 913  
 Shen, C.-J., & Hu, J.-Y. 1999, *Acta Astrophys. Sinica*, 19, 292  
 Siess, L., Dufour, E., & Forestini, M. 2000, *A&A*, 358, 593  
 Simon, M., Close, L. M., & Beck, T. L. 1999, *AJ*, 117, 1375  
 Skinner, S. L., & Yamauchi, S. 1996, *ApJ*, 471, 987  
 Song, I., Bessell, M. S., & Zuckerman, B. 2002, *A&A*, 385, 862  
 Stelzer, B., Huéramo, N., Hubrig, S., Zinnecker, H., & Micela, G. 2003, *A&A*, 407, 1067  
 Sterzik, M. F., & Durisen, R. H. 1995, *A&A*, 304, L9  
 ———. 1998, *A&A*, 339, 95  
 Testi, L., Palla, F., & Natta, A. 1999, *A&A*, 342, 515  
 Testi, L., Palla, F., Prusti, T., Natta, A., & Maltagliati, S. 1997, *A&A*, 320, 159  
 Townsley, L. K., Feigelson, E. D., Montmerle, T., Broos, P. S., Chu, Y.-H., & Garmire, G. P. 2003, *ApJ*, 593, 874  
 Tsuboi, Y., Maeda, Y., Feigelson, E. D., Garmire, G. P., Chartas, G., Mori, K., & Pravdo, S. H. 2003, *ApJ*, 587, L51  
 van den Ancker, M. E., Thé, P. S., Tjin A Djie, H. R. E., Catala, C., de Winter, D., Blondel, P. F. C., & Waters, L. B. F. M. 1997, *A&A*, 324, L33  
 Vieira, S. L. A., Pogodin, M. A., & Franco, G. A. P. 1999, *A&A*, 345, 559  
 Walter, F. M., Alcalá, J. M., Neuhäuser, R., Sterzik, M., & Wolk, S. J. 2000, in *Protostars and Planets IV*, ed. V. Mannings, A. P. Boss, & S. S. Russell (Tucson: Univ. Arizona Press), 273  
 Webb, R. A., Zuckerman, B., Platais, I., Patience, J., White, R. J., Schwartz, M. J., & McCarthy, C. 1999, *ApJ*, 512, L63

- Weinberger, A. J., Rich, R. M., Becklin, E. E., Zuckerman, B., & Matthews, K. 2000, *ApJ*, 544, 937
- Weintraub, D. A. 1990, *ApJS*, 74, 575
- Weisskopf, M. C., Brinkman, B., Canizares, C., Garmire, G., Murray, S., & Van Speybroeck, L. P. 2002, *PASP*, 114, 1
- White, R. J., & Basri, G. 2003, *ApJ*, 582, 1109
- Worley, C. E., & Douglass, G. G. 1997, *A&AS*, 125, 523
- Zinnecker, H., & Mathieu, R., eds. 2001, *IAU Symp. 200, The Formation of Binary Stars* (San Francisco: ASP)
- Zinnecker, H., & Preibisch, T. 1994, *A&A*, 292, 152
- Zuckerman, B., Song, I., Bessell, M. S., & Webb, R. A. 2001, *ApJ*, 562, L87

ERRATUM: “THE  $\epsilon$  CHAMAELEONTIS YOUNG STELLAR GROUP AND THE CHARACTERIZATION  
OF SPARSE STELLAR CLUSTERS” (ApJ, 599, 1207 [2003])

ERIC D. FEIGELSON, WARRICK A. LAWSON, AND GORDON P. GARMIRE

The assignment of the brightest X-ray source to the primary component of the Herbig AeBe systems appears to be incorrect in two cases presented in § 6 and Figure 7 of our original paper. The adopted boresight correction to the HD 141569 field was too large, and the uncorrected X-ray positions indicate that the sources most likely arise from the secondary components HD 141569B and C rather than the primary HD 141569A. The position of the secondary component of HD 150193 is incorrectly plotted in Figure 7; when placed correctly SW of the primary, the most convincing interpretation is that the primary HD 150193A is associated with the fainter X-ray source and HD 150193B with the brighter source. The conclusion in the Abstract that “The *Chandra* observations also increase the census of companions for two of the other four HAeBe stars, HD 141569 and HD 150193. . .” is not correct. The principal results of the study concerning HD 104237 and the  $\epsilon$  Chamaeleontis group of young stars are unaffected by these revisions.

We sincerely thank Beate Stelzer for pointing out these errors. The revised results are discussed in the context of HAeBe X-ray emission by B. Stelzer, G. Micela, K. Hamaguchi, & J. H. M. M. Schmitt (2006, A&A, in press).